BOREAS An international journal of Quaternary research

Landsystem analysis of a tropical moraine-dammed supraglacial lake, Llaca Lake, Cordillera Blanca, Perú

RODRIGO ALBERTO NARRO PÉREZ, CAROLYN H. EYLES, REBECCA E. LEE, LUZMILA DÀVILA RÖLLER AND JOHN C. MACLACHLAN

BOREAS

Narro Pérez, R. A., Eyles, C. H., Lee, R. E., Dàvila Röller, L. & Maclachlan, J. C. 2023 (April): Landsystem analysis of a tropical moraine-dammed supraglacial lake, Llaca Lake, Cordillera Blanca, Perú. *Boreas*, Vol. 52, pp. 272–293. https://doi.org/10.1111/bor.12611. ISSN 0300-9483.

Tropical glaciers of the Cordillera Blanca, Perú are rapidly thinning and retreating as a result of climate warming. The retreat of these glaciers along narrow linear bedrock valleys has increased the number and size of moraine-dammed glacial lakes formed in the valleys. This study aims to identify the geomorphological and sedimentological characteristics of an enlarging moraine-dammed supraglacial lake (Llaca Lake) in the Cordillera Blanca. Field-based sedimentological observations and geomorphological mapping were combined with remotely sensed data and a photogrammetric model derived from aerial surveys by an uncrewed aerial vehicle to identify landform-sediment assemblages. The geomorphological and sedimentological characteristics of Llaca Lake are synthesized into three landsystem zones: Zone 1: distal portions of Llaca Lake and the latero-frontal moraine; Zone 2: the central zone of ice-cored hummocks; and Zone 3: the active glacier margin. These zones are differentiated based on the spatial distribution of landforms, sediments, and active geomorphological processes. This is the first study to describe the landform-sediment assemblages in a tropical moraine-dammed supraglacial lake system and provides a framework for further landsystem element analysis of these growing supraglacial lakes in rapidly deglaciating high-altitude environments.

Rodrigo Alberto Narro Pérez (narrora@mcmaster.ca), Carolyn H. Eyles, Rebecca E. Lee and John C. Maclachlan, School of Earth, Environment and Society, McMaster University, 1280 Main Street West, Hamilton L8S 4K1 Ontario, Canada; Luzmila Dàvila Röller, Instituto Nacional de Investigación en Glaciares y Ecosistemas de Montaña, Av. Centenario 2656 - Sector Palmira, Independencia, Huaraz 02000, Áncash, Perú; *received 31st January 2022, accepted 20th November 2022.*

Glaciers in high-altitude mountain environments, such as the Cordillera Blanca in Perú, are considered some of the most sensitive in their response to climate change and increasing temperatures (Evans & Clague 1994; Huggel *et al*. 2015; Rangwala *et al*. 2015; Emmer *et al*. 2020). Recent climate warming has caused rapid melt of these glaciers (Barnett *et al*. 2005; Silverio & Jaquet 2017; INAIGEM 2018; Hock *et al*. 2019), and an associated increase in the number and size of high-altitude mountain glacial lakes has been documented (Harrison *et al*. 2018; Shugar *et al*. 2020). It is therefore important to understand the geomorphological and sedimentological characteristics of these deglaciating lakes to evaluate how they will be affected by continued glacier recession and also to develop analogues for effective palaeoenvironmental reconstructions of high-altitude regions affected by such changes in the past (e.g. Humlum 1978; Benn *et al*. 2012; Lukas *et al*. 2012; Barr & Lovell 2014; Małecki *et al*. 2018).

Llaca Lake is an enlarging moraine-dammed, supraglacial lake formed at the margin of the Llaca Glacier in the Cordillera Blanca, Perú (Figs 1, 2). This lake is of particular interest as it lies on top of buried glacier ice, which is melting below a cover of supraglacial and lacustrine sediment (Wigmore & Mark 2017) and provides an excellent example of an enlarging moraine-dammed supraglacial lake in a high-altitude setting. Many recent glacier and glacial lake surveys (e.g. Iturrizaga 2014; Harrison *et al*. 2018; INAIGEM 2018; Emmer *et al*. 2020, 2022; Wood *et al*. 2021) identify Llaca Lake as a large lake, yet calculations of water volume in the lake do not account for the volume of water stored in ice buried beneath lacustrine sediments (e.g. Cook & Quincey 2015). The exclusion of this water underestimates calculated lake volumes, which aid in understanding the future development of the lake and its potential water resources that supply the nearby city of Huaraz (Figs 1, 2). Glacial lakes in the Cordillera Blanca take the form of moraine-dammed lakes, debris-dammed lakes, bedrock-dammed lakes, piedmont lakes, supraglacial lakes and a combination of these types (Emmer & Vilímek 2013; Iturrizaga 2014; Emmer *et al*. 2020, 2022). Iturrizaga (2014) states that glacial lakes in the Cordillera Blanca undergo various transition phases between lake types as glaciers retreat. While Llaca Lake may be one of the few ice-contact supraglacial lakes currently in the region, it is possible that many of the lake systems present today may have had supraglacial phases in the past.

Landsystem analysis has been extensively used to document the characteristics of modern glacial environments and to aid in the reconstruction of past glacial processes and environments (e.g. Eyles 1983a; Glasser & Hambrey 2003; Bennett *et al*. 2010; Schomacker *et al*. 2014; Evans *et al*. 2016, 2017; Lee *et al*. 2018). A similar landsystems approach has been used to document the geomorphological record of a retreating cirque

DOI 10.1111/bor.12611

glacier elsewhere in the Andes (Małecki *et al.* 2018) and to document geomorphological processes on debris-covered glaciers in the Himalayas (Owen *et al.* 2009; Benn *et al.* 2012), Karakoram (Owen & Derbyshire 1989) and Alps (Stefaniak *et al.* 2021). It is also anticipated that with glacier recession, water supply to local communities in the Cordillera Blanca will be severely reduced, as has occurred in the Himalayas (Lee *et al.* 2021), and the storage capacity of glacial lakes such as Llaca Lake will need to be carefully evaluated (Watson *et al.* 2016; Irvine-Flynn *et al.* 2017; Mark *et al.* 2017).

This study aims to identify the geomorphological and sedimentological processes operating in Llaca Lake using a landsystems approach and provide a base-level understanding of conditions that are predicted to change as glaciers continue to recede due to climate warming. Investigation of the geomorphological and sedimentological characteristics of Llaca Lake will also allow landform characteristics to be linked with underlying sediment to provide insight into former depositional processes. This study will also help to better understand how lake volumes and potential water resources may change in the future.

Study area

Andean tropical glaciers and climate change

Tropical glaciers in the Andes are shrinking at a considerable rate (Silverio & Jaquet 2017; INAIGEM 2018; Małecki *et al.* 2018; Veettil 2018; Vuille *et al.* 2018). In Perú, which lies in the outer tropics,

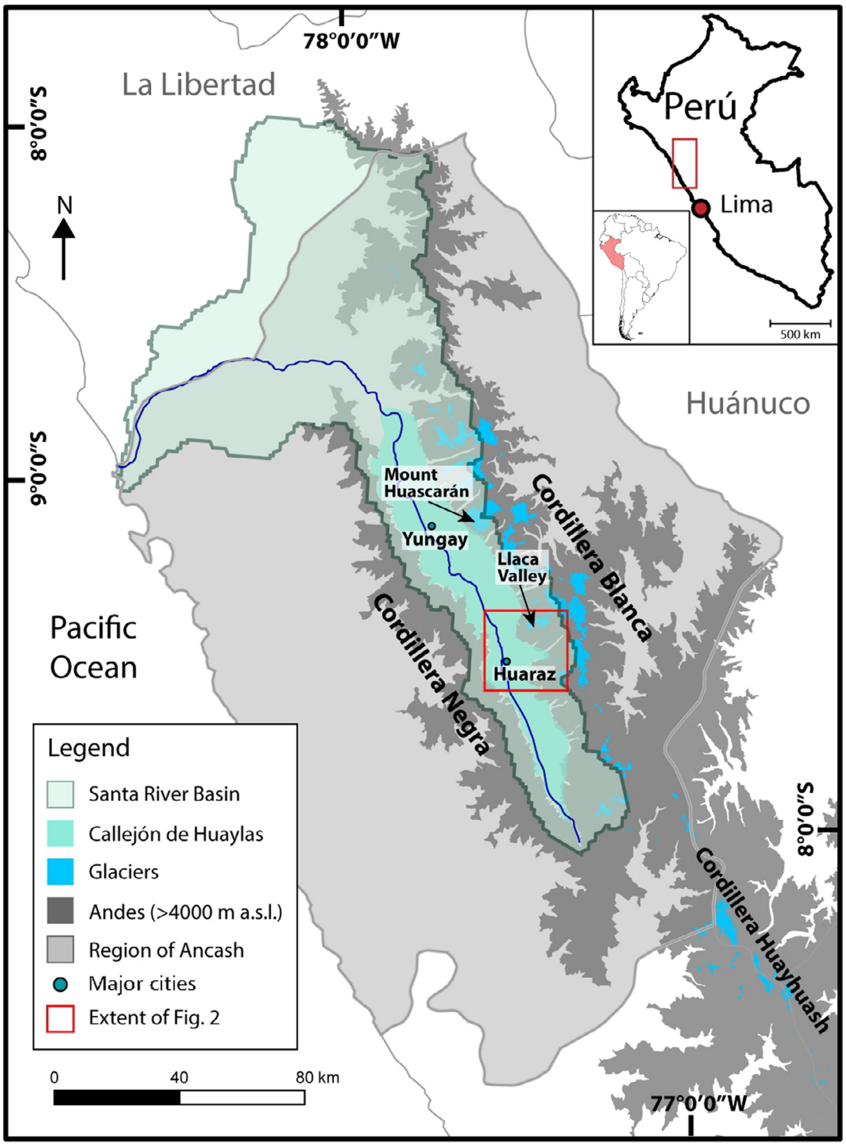

Fig. 1. Location of Llaca Valley within the Cordillera Blanca, close to the city of Huaraz, shown in the red box (Fig. 2).

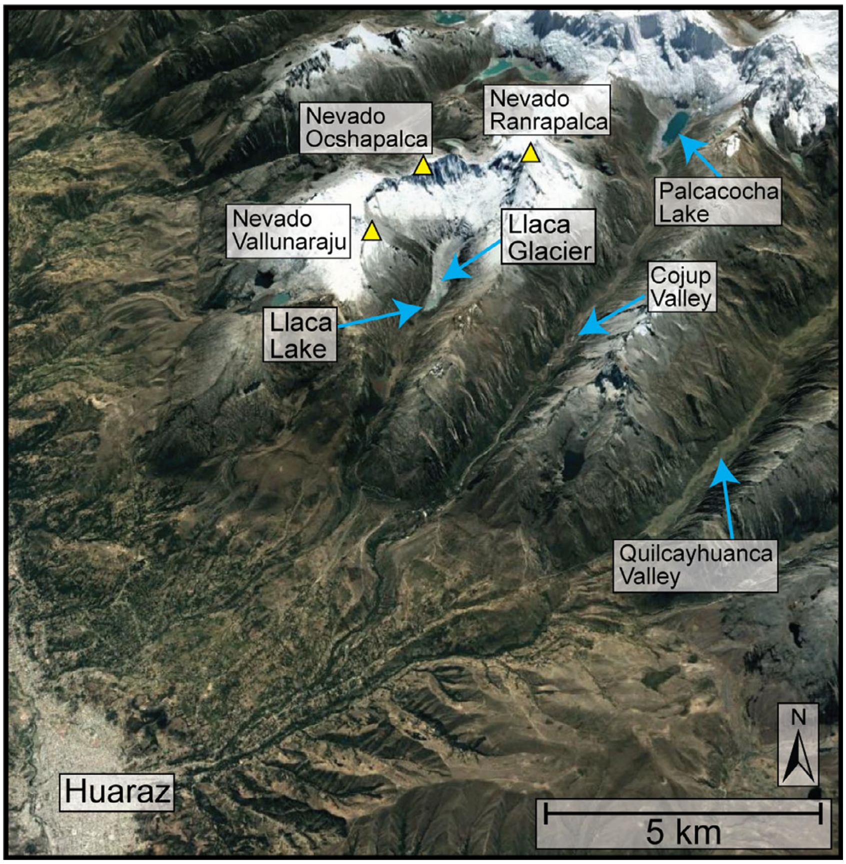

Fig. 2. Location of Llaca Lake, Llaca Glacier and surrounding mountains. The Cojup Valley, Palcacocha Lake, Quilcayhuanca Valley and the city of Huaraz are also shown on this map. Location of this map within the Cordillera Blanca is shown by the red box in Fig. 1.

precipitation is generally considered to have the strongest influence on glacier mass balance (Vuille *et al*. 2008) and occurs mostly in the wet season between November and March (Kaser 2001; Rabatel *et al*. 2013; Veettil *et al*. 2017). A delayed wet season will lead to high ablation rates as the low albedo of the mostly debris-covered glacier surface at the end of the dry season causes high rates of absorption of solar radiation and enhanced melting. However, since there is no evidence to suggest that precipitation amounts have decreased during the 20th century, it is likely that increased average annual temperatures are the main cause for the documented shrinking of the Andean cryosphere (Vuille *et al*. 2003, 2008; Rabatel *et al*. 2013). Analysis of data from over 100 weather stations in the Cordillera Blanca has identified an annual average air temperature increase of about 0.31 °C per decade between 1969 and 1998, and of 0.13 °C per decade from 1983 to 2012 (Mark & Seltzer 2005; Schauwecker *et al*. 2014). This average temperature increase has greatly enhanced melting of glaciers in the Cordillera Blanca (Barnett *et al*. 2005), decreasing the total glaciated area from 800–850 km^2 in 1930 to 448.81 km^2 in 2016 (Georges 2004; INAIGEM 2018) and having most impact on small, low-elevation glaciers that are extremely sensitive to climate change (Schauwecker *et al*. 2014).

Cordillera Blanca

The Cordillera Blanca is a 250-km-long mountain range that lies within the Peruvian Cordillera Occidental and contains one of the largest tropical glaciated areas in the world (Fig. 1; Mark *et al*. 2010; Lynch 2012; Bury *et al*. 2013; INAIGEM 2018; Vuille *et al*. 2018). The majority of mountain summits within the Cordillera Blanca lie between 5000 and 6000 m a.s.l., with several reaching over 6000 m a.s.l. in the northern and central parts of the mountain range (Deverchère *et al*. 1989; Margirier *et al*. 2016). Nevado Huascarán, in the central part of the Cordillera Blanca, is the highest summit reaching an altitude of 6757 m a.s.l. (Margirier *et al*. 2016; INAIGEM 2018). Granodiorites of the Cordillera Blanca Batholith (emplaced approximately 14–5 Ma; McNulty & Farber 2002; Margirier *et al*. 2016) form the dominant geological units in this region and intrude into shales and sandstones of the Upper Jurassic Chicama Formation (Schwartz 1988; Margirier *et al*. 2016, 2018). The Cordillera Blanca Batholith has been deeply incised by glaciers during the Quaternary creating the deep, U-shaped glacial valleys prominent throughout the mountain range (Clapperton 1972; Rodbell 1992; Smith *et al.* 2005).

As the glaciers of the Cordilla Blanca rapidly retreat, the previously glaciated valleys and deeply scoured basins they contain are quickly infilled by glacial meltwater, creating a variety of ice contact and non-ice contact glacial lakes (Fig. 2). The first inventory of glacial lakes in the Cordillera Blanca, compiled in 1951, identified 230 lakes of 'significant size' (Concha 1951; Emmer *et al.* 2016); the most recent national inventory (2014) reports over 1902 glacial lakes in the Cordillera Blanca, 830 of which have a surface area greater than 5000 m^2 (Tacsi Palacios *et al.* 2014). Vilímek *et al.* (2016) identified 2370 lakes of all sizes in the Cordillera Blanca; Emmer *et al.* (2016) used the same data source to identify 882 lakes of 'significant size' (lake width >20 m and lake width plus lake length >100 m). The most recent lake inventory (Emmer *et al.* 2020) determined that ~643 lakes existed in 1948 and ~893 lakes in 2017; total lake area also increased from approximately 29 km^2 in 1948 to 35 km^2 in 2017.

A major concern is that many of these glacial lakes are impounded by large, often unstable, latero-frontal moraines that act as naturally occurring dams (Kershaw *et al.* 2005; Vilímek *et al.* 2005; Emmer & Vilímek 2013; Miles *et al.* 2018); in the Cordillera Blanca, approximately 48% of large lakes (>100 000 m^2) have been characterized as moraine-dammed (Emmer *et al.* 2016, 2020; Harrison *et al.* 2018). Displacement of proglacial lake water caused by various mechanisms such as landslides, rockfalls or icefalls, can lead to moraine dam breach and the sudden release of water as glacial lake outburst floods (GLOFs). These floods can be catastrophic to communities living downvalley of the moraine impounded lakes (Carey 2005; Hubbard *et al.* 2005; Kershaw *et al.* 2005; Emmer *et al.* 2016, 2022). In 1941, a catastrophic flood released by failure of the moraine dam of Lake Palcacocha took the lives of 1800 people in and around the city of Huaraz (Carey 2005; Wegner 2014). Since this event, the water levels in many lakes within the Cordillera Blanca have been monitored and remediation efforts have strengthened the moraine dams of approximately 40 lakes (Emmer *et al.* 2018); efforts have also been made to predict and model the occurrence of these hazardous GLOF events (Klimeš *et al.* 2009, 2014; Carey 2010; Carey *et al.* 2012; Portocarrero 2014; Schneider *et al.* 2014; Emmer *et al.* 2016, 2022; Somos-Valenzuela *et al.* 2016; Mergili *et al.* 2020).

Llaca Glacier and Llaca Lake

Llaca Glacier is situated at the head of the Llaca Valley, a linear and relatively narrow valley (~500 m) that extends from a cirque bordered by Nevado Vallunaraju (5686 m a.s.l.) in the west, Nevado Ocshapalca (5888 m a.s.l.) in the north and Nevado Ranrapalca (6162 m a.s.l.) in the east (Fig. 2; Torres Amado *et al.* 2016). The tributary glaciers Ocshapalca and Ranrapalca extend into the valley to join as Llaca Glacier, which terminates in Lake Llaca at an elevation of ~4500 m a.s.l. Supraglacial debris, sourced from the steep valley walls and lateral moraines that surround the glacier, covers much of the glacier surface and is >1 m thick at its terminus in Llaca Lake (Wigmore & Mark 2017). Llaca Lake lies in contact with the active ice margin, overlies stagnant glacier ice in the basin, and is impounded by a large latero-frontal moraine (Wigmore & Mark 2017; Figs 3, 4). This supraglacial moraine-dammed lake is approximately 1 km long (Figs 5, 6) and lies approximately 14 km northeast of the city of Huaraz (Fig. 2). The water that flows from Llaca Lake is part of the sub-basin Casca that drains into the larger Santa River, the most important freshwater river in the region (Figs 1, 3; Torres Amado *et al.* 2016).

In 1973, Llaca Lake was reported to have a volume of 794 000 m^3 and an area of 63 312 m^2 (Torres Amado *et al.* 2016; ANA 2020). In an effort to mitigate the potential for a GLOF, a 10-m-high, concrete-veneered earth dam was constructed in 1977 to control outflow and lower lake levels (Fig. 3; Portocarrero 2014). In 2004, a new survey indicated the lake to have a reduced volume of 274 305 m^3, an area of 43 988 m^2, and a maximum depth of 16.8 m (Torres Amado *et al.* 2016). Estimates of the lake size made in 2017 show the lake has since expanded due to glacier margin retreat and now has a volume of 495 477 m^3, an area of 65 513 m^2, and an approximate dam freeboard of 14 m (Figs 3, 4; INAIGEM 2018; Muñoz *et al.* 2020). The processes currently operating within Llaca Lake have therefore been influenced by recent human modifications to the outflow and controls on water depth. However, the dams and outflow systems of several other lakes at risk of generating destructive GLOFs in the Cordillera Blanca have been modified in a similar fashion (Emmer *et al.* 2018) and the processes operating in Llaca Lake are likely representative of those operating in these modified lakes.

As with most glaciers in the Cordillera Blanca (Silverio & Jaquet 2017; INAIGEM 2018), Llaca Glacier has undergone significant marginal retreat and loss of mass over the past several decades. Between 2005 and 2019, the active glacier margin retreated between 250 and 330 m (Fig. 4). It is not known exactly when ice stagnated in the basin now covered by Llaca Lake but the presence of Llaca Lake as a body of water was first reported in 1973 (Torres Amado *et al.* 2016). The lake began to form and grow as the underlying stagnant ice progressively melted; this dynamic process can be clearly seen on satellite imagery of the region taken between 2005 and 2019 (Fig. 4). Differential melting of stagnant ice buried beneath the water and sediment cover has

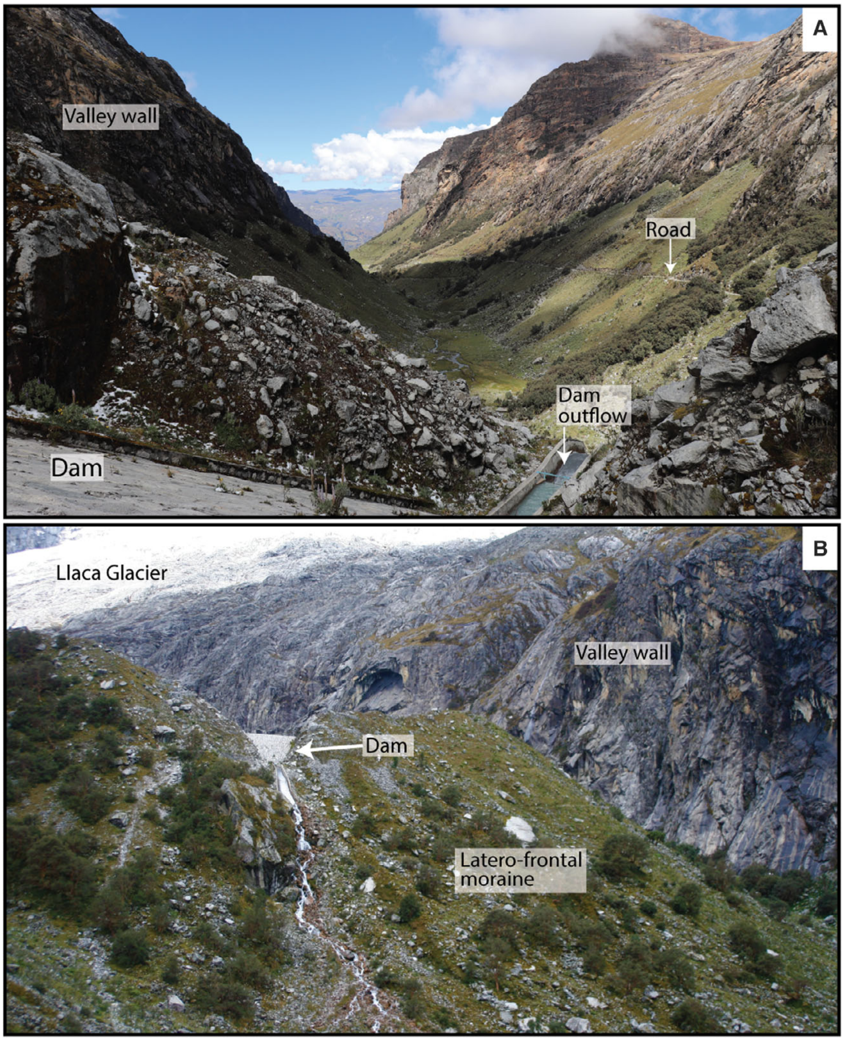

Fig. 3. A. Downvalley view of Llaca Valley from the top of the Llaca Dam. Coarse-grained debris comprising the latero-frontal moraine is visible on the left side of the image. Note the constructed dam and outflow channel, which were emplaced to reduce the risk of dam breaching. B. View upvalley of the Llaca Lake dam (the dam is approximately 14 m high). Llaca Lake lies between the dam and Llaca Glacier in the background. Satellite image from Google Earth V. 7.3.4.8248 (2019).

created a constantly changing topography of exposed ice-cored hummocks and water-filled basins (Fig. 4; Iturrizaga 2014). Lacustrine sediments exposed on the surface of hummocks provide important information regarding the nature of sediments accumulating beneath the water surface in such supraglacial lake basins.

Material and methods

This study involves the integration of remotely sensed data with field-based sedimentological observations and geomorphological mapping. Google Earth satellite imagery (Google Earth 2005, 2011, 2013, 2016, 2017, 2019) was utilized to provide high resolution images (<0.5 m) that allowed identification of geomorphological features within Llaca Lake and documentation of their changes over time (Fig. 4). Vector shapefiles (points, lines and polygons) of these surface features were created on Google Earth for each of the data sets available for selected years between 2005 and 2019 and were imported into ArcMap for analysis of their dimensions (Figs 4, 5).

Fieldwork at Llaca Lake was conducted during May 2017 and May 2019 and included the observation and measurement of sedimentological and geomorphological features and the completion of aerial surveys by an uncrewed aerial vehicle (UAV). The locations of logs recorded from sedimentary lithofacies exposed in hummocks on the ice surface and in two excavated pits on the lake margin are shown in Fig. 6. Sedimentary lithofacies were photographed and logged using standard sedimentological techniques recording field-estimated particle size (texture), clast shape, bed contacts, sedimentary structures and/or deformation structures (Eyles *et al.* 1983).

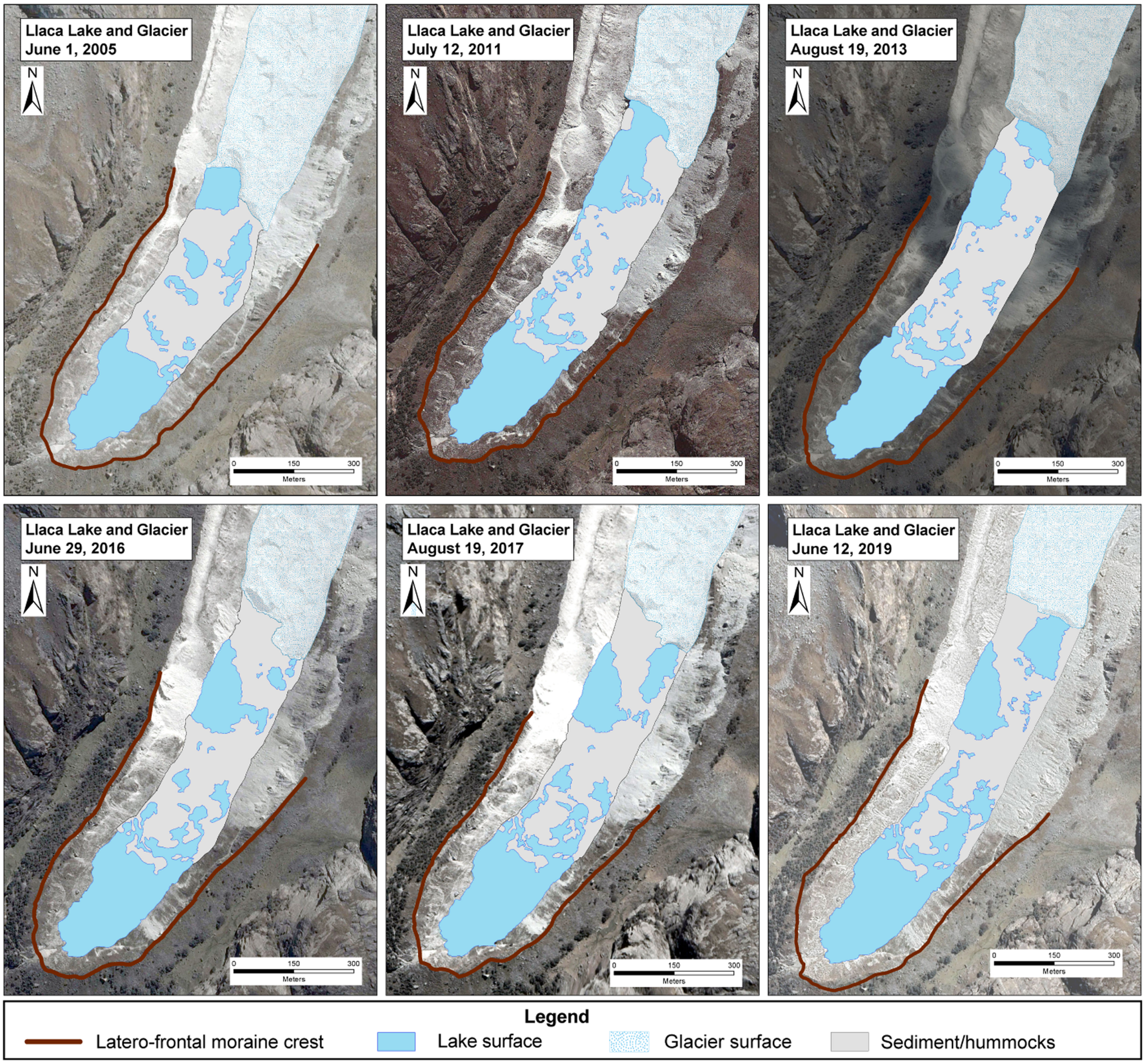

Fig. 4. Mapped satellite imagery showing changes in the distribution of lake water and exposed sediment/ice-cored hummocks in Llaca Lake as Llaca Glacier receded between 2005 and 2019. Satellite imagery from Google Earth (Google Earth 2005, 2011, 2016, 2017, 2019).

To allow a more complete analysis of the geomorphology of Llaca Lake and its associated landforms and sediments, a DJI Phantom 4 Advanced UAV was used to complete five photogrammetric aerial surveys of the Llaca Lake region, covering a total area of approximately 2 km^2 with 1305 images. The aerial surveys were conducted at 50–60 m above the ground surface, depending on proximity to the surrounding valley walls and obstacles to the flight path, resulting in a pixel resolution of 5 cm. Eighteen ground control points (GCPs) were established in accessible locations using a portable GPS (SXBlue GNSS); these GCPs had a precision of ~1 m and allowed georectification of the photogrammetric point cloud generated from UAV surveys. The Pix4d Capture app was utilized to automate flight paths and to ensure that image spacing was consistent with an overlap of between 80 and 90%. A model of the study area was created from the photogrammetric imagery using Agisoft Metashape Professional software version 1.6.5 (Fig. 6). Data processing of the imagery followed a standard structure from motion (SfM) workflow (Gauthier *et al.* 2015; Evans *et al.* 2016; Ely *et al.* 2017). For each of the surveys, images were inputted into Metashape as a single mosaic unit and aligned. The number of points analysed was 448 505 124, with an average surface density of 760 points m^{-2}, and average point spacing of 0.036 m. Ground control points (GCPs) were identified on the

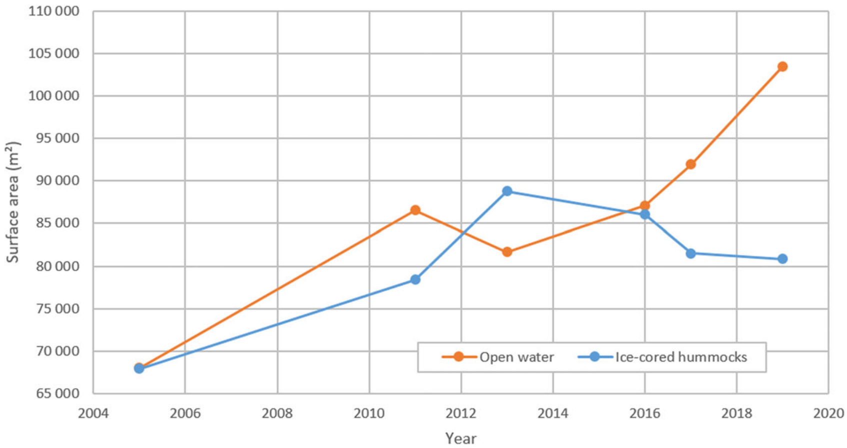

Fig. 5. Surface area changes in ice-cored hummocks and open water for Llaca Lake between 2005 and 2019.

images and the images were aligned again, using the GCPs to increase accuracy. The final set of aligned points was refined, removing any points with a reprojection error greater than 2.5 cm (0.5 pixels), and was used to create a dense point cloud. From the dense point cloud, a mesh, DEM and orthophoto were created to be used in the analysis, each with a resolution of 5 cm. However, it must be acknowledged that SfM processing can incorporate errors associated with GCP and drone GPS inaccuracies, as well as errors caused by changing light conditions during the survey.

The sedimentological and geomorphological data were combined to determine process-form relationships within the Llaca Lake landsystem and to identify landsystem elements. A geomorphological map of the landsystem elements was created using data from the model developed from the UAV survey, field observations, and recent aerial imagery (ESRI 2019; Google Earth 2019; Fig. 8). Landform elements were then grouped into landsystem zones, which are the product of spatially differentiated processes operating within the landsystem (Eyles 1983a; Evans 2003). Landsystem analysis is a powerful tool that has been used in a range of glacial environments to understand both modern glaciers and ice sheets and for palaeoglacial reconstruction (Evans *et al*. 1999, 2016, 2017; Evans 2003; Fitzsimons 2003; Glasser & Hambrey 2003; Schomacker *et al*. 2014; Stokes *et al*. 2015; Małecki *et al*. 2018; Chandler *et al*. 2020). By linking the geomorphology of the terrain with its subsurface material and depositional processes, the delineation of glacial landsystems also allows for subsurface conditions to be predicted from surface morphological features.

Geomorphological characteristics of Llaca Lake

Geomorphological mapping of surface landforms identified from Google Earth imagery and from the DEMs and orthomosaic model created from the UAV survey allowed delineation of eight landsystem elements (Fig. 7). These elements include the valley walls, outer moraine valley trough, rockfall and avalanche fans, the latero-frontal moraine damming the lake, the debris-covered glacier tongue, moraine slope failures, ice-cored hummocks, and alluvial fans.

Valley walls

Valley walls that enclose the Llaca Lake landsystem are composed of granodiorite (Cobbing *et al*. 1981; Giovanni *et al*. 2010) and are subject to a variety of mass wasting processes including rockfalls and rockslides. The Llaca Valley is relatively narrow, ranging from 500–800 m wide (Figs 2, 7) and has a northeast–southwest orientation (Wigmore & Mark 2017). At the narrowest part of the valley, around the position of the front of the latero-frontal moraine, valley walls are extremely steep (ranging from 68° to 83°); as the valley widens towards the active glacier face, the valley walls are less steep (approximately 57°–77°). These steep valley rockwalls are the primary sediment source for rockfalls and debrisflows and contribute a significant amount of debris into the Llaca Lake system (Fig. 7).

Outer moraine trough

The outer moraine trough is located between the valley walls and the distal slope of the latero-frontal moraine and is vegetated by grasses, small shrubs, and trees (Fig. 7). The width of the trough varies from 20 to 150 m, and it generally widens in the downvalley direction; the western valley trough is narrower than the eastern valley trough (Fig. 8). The outer moraine trough acts as a gutter, trapping debris and sediment from rockfall debris. Rockfall and avalanche fans that supply coarse material to the trough floors are also present, particularly along the eastern moraine valley trough (Fig. 5).

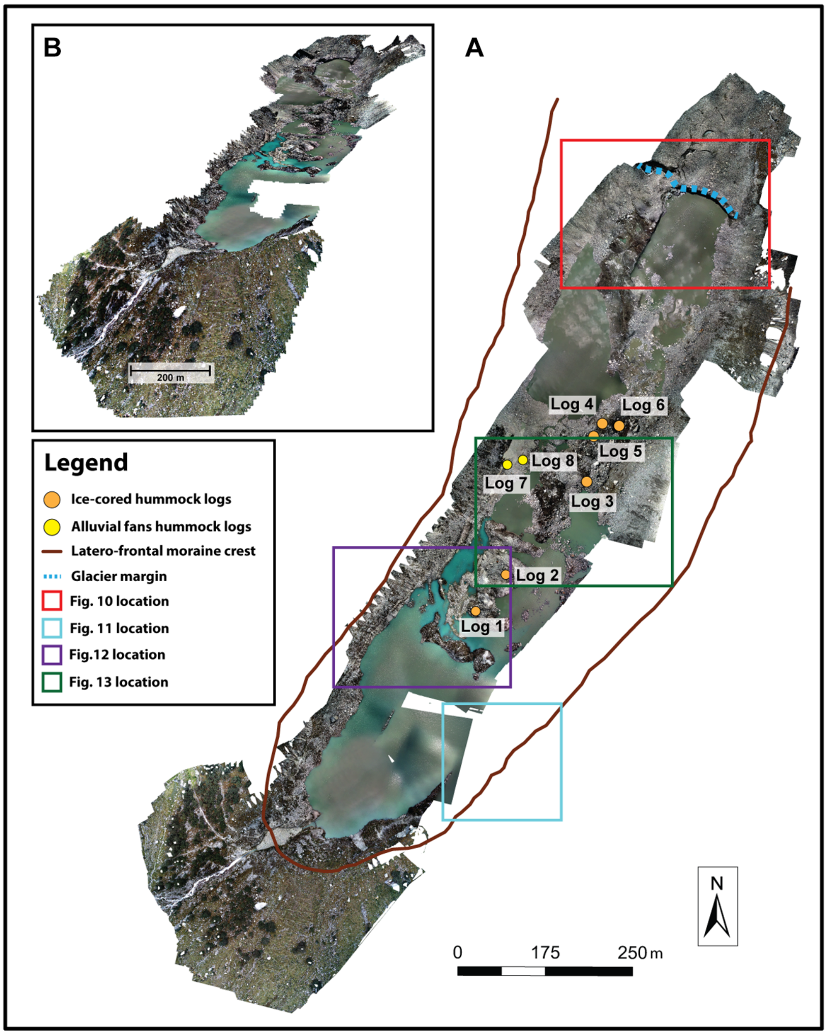

Fig. 6. A. Orthomosaic of Llaca Lake created from UAV photogrammetry (2019) showing the frontal section of the latero-frontal moraine and the margin of Llaca Glacier (upper right). Location of sedimentary logs recorded from excavations in ice-cored hummocks is indicated by the orange dots; the location of sedimentary logs recorded from pits excavated on alluvial fans is indicated by yellow dots. Resolution of orthomosaic model is 5 cm. B. Orthomosaic model overlaid on a 5 cm DEM.

Latero-frontal moraine

Approximately 60–80 m in height and with varying widths of between 150–300 m, the large latero-frontal moraine (Figs 3, 4, 8) that currently impounds Llaca Lake is an imposing geomorphological feature. The latero-frontal moraine passes upvalley into lateral moraines fringing the current glacier margins (Figs 3, 4). The northwestern side of the latero-frontal moraine is well vegetated with shrubs, trees and grasses; vegetation is sparse on the southeastern side of the moraine, although small clusters of trees grow on the ridge between the latero-frontal moraine and valley wall (Fig. 6).

An exposure (~95 m in width by ~30 m in height) through the northern lateral moraine shows crude stratification of sediments ranging from matrix supported diamicts to gravel horizons and boulders 3–8 m in diameter (Fig. 8). The discontinuous gravel horizons, 10–30 m in length, dip in a SW direction, away from the ice margin and impart a crude stratification to the exposure (Fig. 8). Such large lateral and frontal moraines commonly consist of poorly sorted sediments of glacial or glacially transported origin, deposited by a variety of processes including debris falls, slumps, and slides from supraglacial and englacial sources (Owen & Derbyshire 1989; Benn *et al.* 2003; Bowman *et al.* 2018). The internal structure of the lateral moraine fringing Llaca Lake suggests that the moraine may have formed in a similar way, from the alternating accumulation of sediment supplied by supraglacial debrisflows and falls from the lateral ice margins (Kirkbride & Spedding 1996;

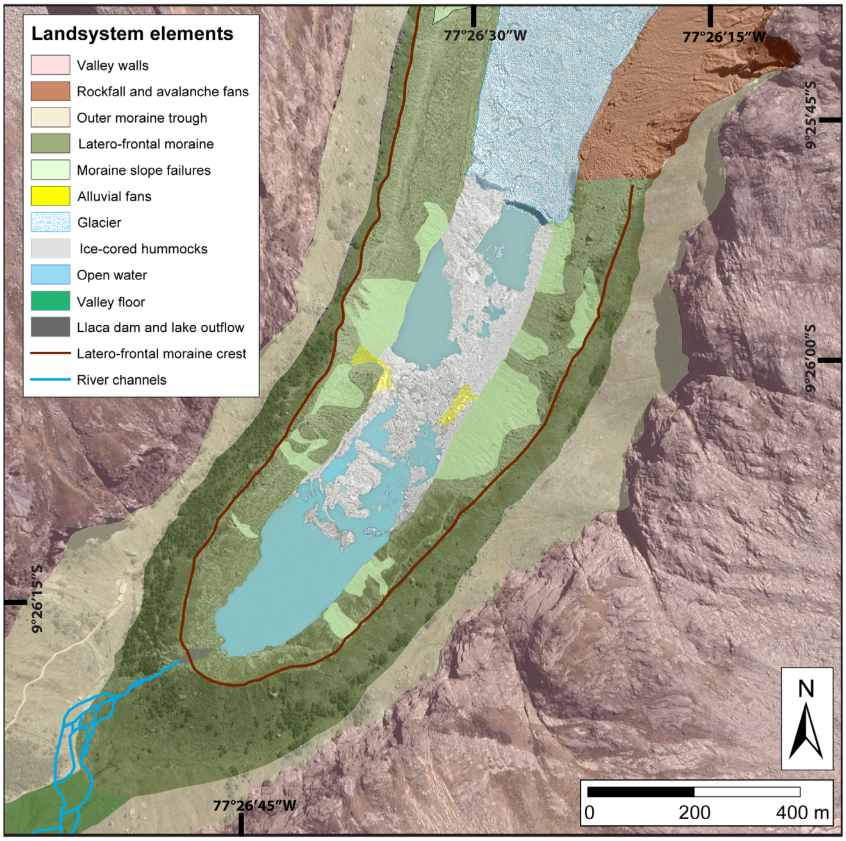

Fig. 7. Landsystem element map based on data compiled from the 2019 UAV survey and orthomosaic model, field observations, and recent aerial imagery (ESRI 2019; Google Earth 2020).

Benn & Owen 2002; Sigurðardóttir 2013). A very similar latero-frontal moraine that impounds Palcacocha Lake in an adjacent valley (Fig. 2) contains interbedded massive gravels (Gms) and matrix-supported diamicts deposited by debrisflows and the reworking and bulldozing of debris at the glacier front (Bowman *et al.* 2018). While distinct local factors may have played a role in moraine formation, it is possible similar moraine building processes occurred in the Llaca Valley.

Rockfall and avalanche fans

Large rockfall and avalanche fans (>100 m in length) are generated by the down-slope transport of large amounts of coarse-grained debris from the valley walls onto the glacier surface and into the valley (Figs 7, 9A, B). Close to the active glacier margin, rock failures originate from the adjacent valley walls and contribute debris to both lateral moraines and the lake basin. Rockfall and avalanche fans are also present on the margins of the outer moraine valley troughs (Fig. 4).

Debris-covered glacier tongue

The active tongue of Llaca Glacier terminates as a steep, debris-covered ice cliff in the northeastern portion of Llaca Lake (Wigmore & Mark 2017; Fig. 9A). The combination of high relief and frequent rockfalls and avalanches, triggered by events that include earth movements associated with ongoing tectonic uplift of the region, ensures that the tongue of Llaca Glacier is debris-covered (Fig. 9A, B). This debris is typically dominated by angular clasts, with large boulders reaching up to several metres in diameter. As the ice cliff undergoes backwasting, this coarse-grained supraglacial debris is deposited into the lake basin (Fig. 9). The receding glacier tongue can be either in direct contact with the open water of the lake (e.g. Fig. 9A, D), or covered by variable thicknesses of supraglacial debris (e.g. Fig. 10B). The presence of this debris, combined with the many dynamic sedimentary processes operating in the region of the glacier tongue (e.g. sediment gravity flows, surface water flows) often make it difficult to determine the exact location of the active ice margin.

Moraine slope failures

There is abundant evidence to indicate intermittent failure of the steep moraine slopes bordering Llaca Lake (Figs 6, 9). These slope failures form coarse-grained sediment aprons, smaller (50–90 m in length) than the large rockfall and avalanche fans found upvalley and are

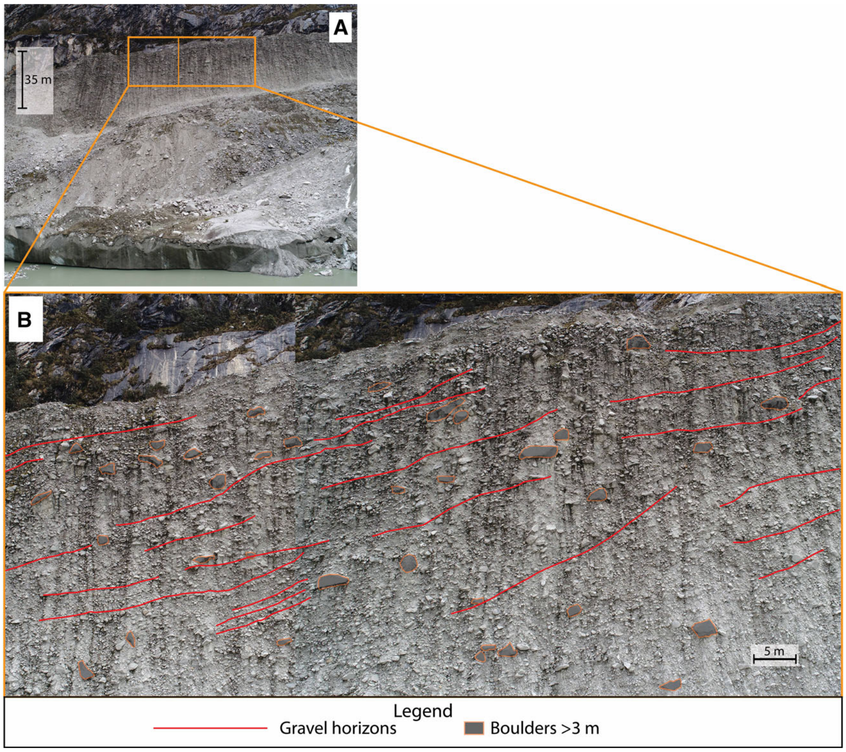

Fig. 8. A. Section of the lateral moraine along the northern boundary of Llaca Lake. Orange box shows position of photomosaic images shown in B. B. Photomosaic image of part of the northern lateral moraine of Llaca Lake showing crudely stratified, poorly sorted sediments, ranging from fine sediments to large boulders 3–8 m in size, and boulder horizons dipping towards the SW (towards left of image).

common along the base of the latero-frontal moraine surrounding Llaca Lake (Fig. 9B–D). Moraine slopes in the ice-distal (southwestern) section of the lake are often vegetated (with mosses and shrubs); removal of this vegetation when a failure event occurs allows the slope failure to be easily identified (Fig. 11).

Ice-cored hummocks

Large ice-cored sediment hummocks are found throughout the area of Llaca Lake (Figs 9, 10). It is estimated that in 2005 the ice-cored hummocks had a surface area of approximately 67 927 m^2 and reached a maximum of 88 808 m^2 in 2013; this has since been decreasing to an estimated area of 80 860 m^2 in 2019 (Fig. 5). The hummocks are created through differential melting of buried ice beneath the thick cover of lacustrine and supraglacial material that covers and insulates the decaying ice (Lukas 2008; Bennett *et al*. 2010). Sediments exposed in the hummocks are mostly composed of either large angular or subangular boulders of supraglacial origin (Fig. 9) or laminated fine-grained silts and fine sands deposited under lacustrine conditions (Fig. 9). Some of the surficial debris present on the hummocks may also have been supplied by inflowing streams or the failure and transport of sediment from the steep and unstable moraine walls surrounding the lake. Variable thicknesses of supraglacial debris covering the buried stagnant ice permit differential rates of ablation and melting, creating a chaotic and constantly changing hummocky topography within the lake basin (Figs 9, 10; Nicholson *et al*. 2018). The most ice-distal region of ice-cored hummocks was significantly reduced in areal extent by ~45% between 2005 and 2019 (Figs 5, 12), but the overall form and location of the ice-cored region remained relatively uniform. In comparison, the ice-cored hummocks in the central section of the lake show a high degree of variability in the extent and form of the hummocks and associated open water bodies (Fig. 13). The progressive changes in the topography of this region strongly suggest the continual melt of buried ice and progressive subsidence of the debris-covered ice surface. Buried ice can also be observed in exposures through the hummocks close to the glacier margin (Fig. 9C, D) and the hummocky surface topography elsewhere suggests that stagnant ice likely underlies most of the lake basin. The sedimentary facies present in these ice-cored hummocks (Figs 14, 15) are described in detail in the following section.

Alluvial fans

Alluvial fans generated by surface water flows transporting and reworking unstable sediment along the inner side of the lateral moraines, form fan-shaped bodies lying between Llaca Lake and the lateral moraines (Figs 8, 9B,

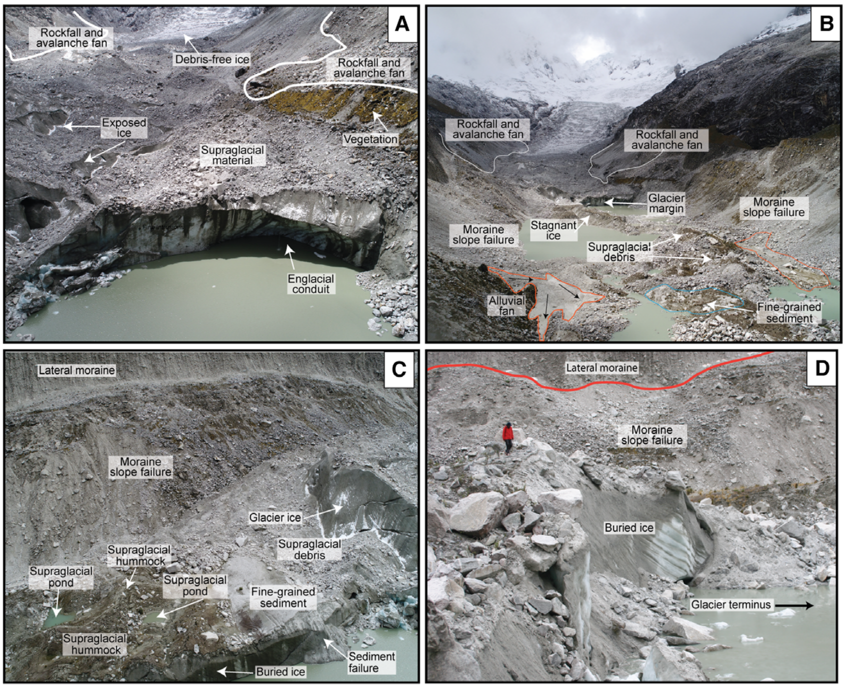

Fig. 9. A. Annotated photograph of the margin of Llaca Glacier showing cover of supraglacial debris, exposed glacier ice and rockfall and avalanche fans. B. Upvalley view of Llaca Lake and Llaca Glacier. Alluvial fans entering the lake are outlined in orange; fine-grained sediment exposed on ice-cored hummocks is outlined in blue. C. Ice-cored hummocks overlain by coarse, angular supraglacial debris. D. Supraglacial sediment on top of buried ice.

16). Sediments exposed in these fans are characterized by massive sand with pebbles (Sm, Gm; Fig. 16B, D) deposited from the episodic rapid influx of sediment and are interbedded with occasional silt horizons.

Sedimentological characteristics

The sedimentary characteristics of two accessible elements of the Llaca Lake landsystem are described here

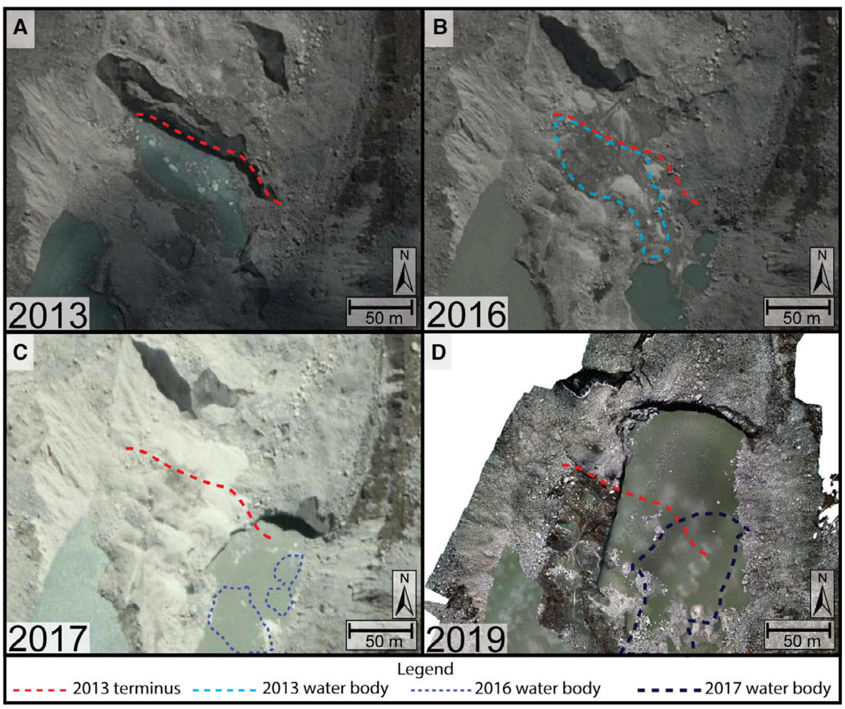

Fig. 10. Changes in the Llaca Glacier debris-covered glacier tongue and ice proximal lacustrine environments between 2013 and 2019.

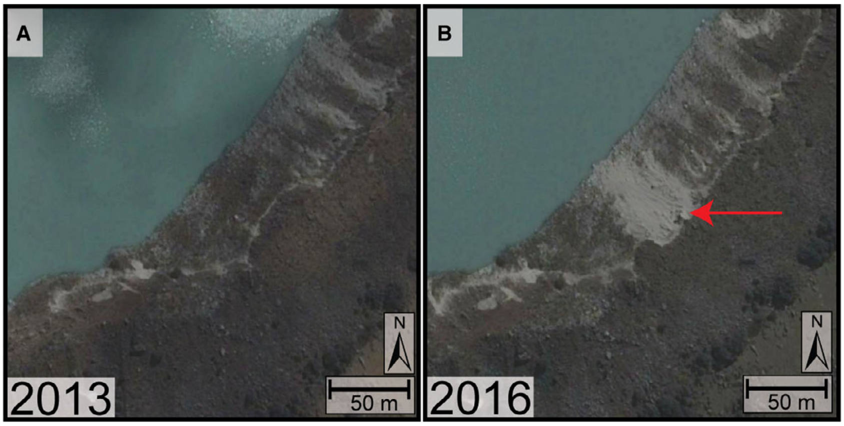

Fig. 11. Moraine slope failures occur along the inner side of the latero-frontal moraine and transport sediment into the lake. A moraine slope failure that occurred at some time between 2013 (A) and 2016 (B) is recorded by satellite images taken in 2016 (red arrow; Google Earth 2013, 2016).

and include sediment exposed on the margins of ice-cored hummocks (Logs 1–6; Fig. 15) and in pits dug into an alluvial fan (Logs 7 and 8; Fig. 16). Eight lithofacies types (Fig. 14) were identified in these exposures including laminated fines (Fl), deformed fines (Fd), horizontally bedded sand (Sh), massive sand (Sm), graded sand (Sg), rippled sand (Sr), deformed sand (Sd) and massive gravel (Gm).

Ice-cored hummocks (Logs 1–6; Fig. 15)

Fine-grained facies. – Fine-grained facies dominate the sediments exposed on ice-cored hummocks (Fig. 9B–D). Very fine-grained sand, silt and clay are grouped together as fine-grained facies and include laminated silts and clays (Fl; Fig. 14I), deformed units of silt and clay (Fd; Fig. 14J), and interbedded horizontally laminated sand (e.g. Sh, Fl; Fl, Sh; Fig. 14B, J). Deformed fine-grained facies (Fd) contain soft sediment deformation structures (folds) and brittle deformation structures in the form of microfaults (Fig. 14J). The thickness of deformed beds varies from 2 to 70 cm.

Fine-grained facies are interpreted as the product of deposition from overflows, interflows, and suspension settling of fine-grained sediment supplied by meltwater into the waters of Llaca Lake (e.g. Eyles & Clark 1988; Eyles 1993; Chikita *et al*. 2001; Evans *et al*. 2010; Eyles & Eyles 2010). Laminated facies record changing supply mechanisms and energy levels in the lake; deformed facies (Fd; Fig. 14J) record disruption of the sediment by water escape and/or slumping as underlying ice melts and sediment fails down-slope (e.g. Eyles 1979). Ductile

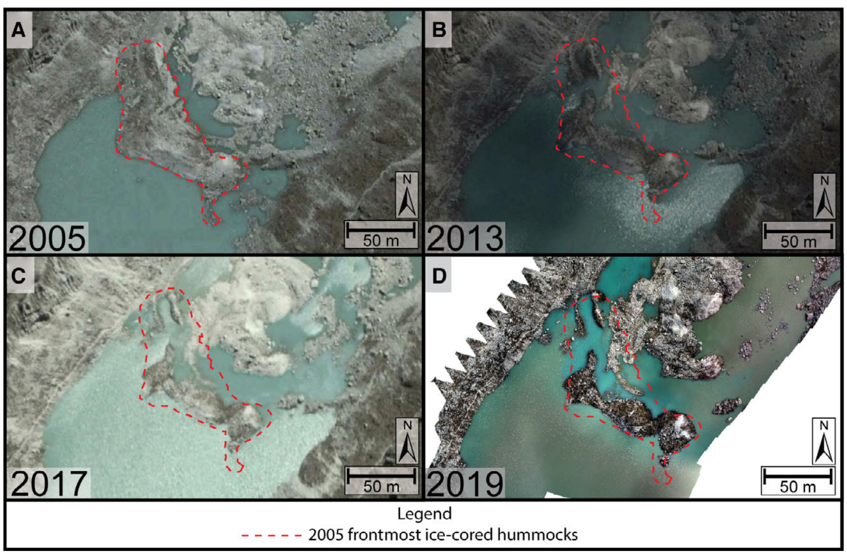

Fig. 12. Change in size and shape of exposed ice-cored hummocks in the most ice-distal region of Llaca Lake between 2005 and 2019. Satellite imagery for the years 2005, 2013, 2017 is from Google Earth (Google Earth 2005, 2013, 2017). The 2019 image is from the model created in this study.

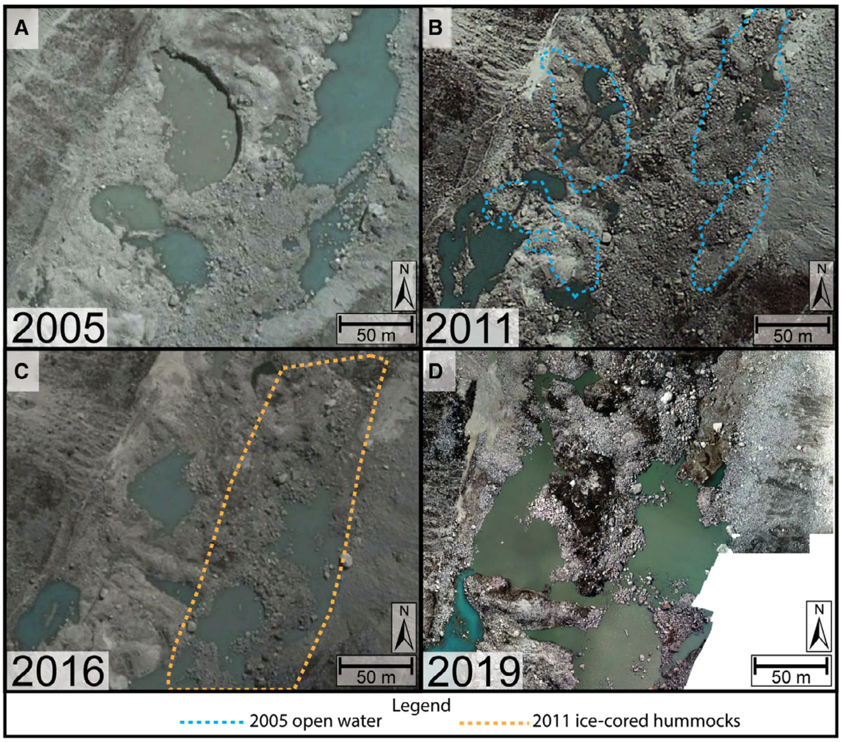

Fig. 13. Ice-cored hummocks and water filled depressions in the central section of Llaca Lake between 2005 and 2019. Satellite imagery for 2005, 2011 and 2016 is from Google Earth (Google Earth, 2005, 2011, 2016). 2019 image (D) derived from UAV photogrammetry of this study.

deformation in these facies may also be the result of overpressuring caused by rapid deposition of overlying sediment and readjustments of the sediment pile (Eyles *et al*. 1987).

Coarse-grained facies. – Scattered angular clasts and a variety of sand facies are also exposed on the ice-cored hummocks. Angular clasts up to 1 m diameter are commonly found on the upper surface of hummocks and may be surrounded by finer-grained sand or silt (Fig. 14K). Sand facies consist of horizontally bedded fine- to medium-grained sand (Sh; Fig. 14B), massive (structureless) fine- to medium-grained sand (Sm; Fig. 14B, C), graded fine- to medium-grained sand (Sg; Fig. 14D), rippled sand (Sr; Fig. 14E), and fine- to medium-grained deformed sand (Sd). Deformed sand facies show evidence of both brittle deformation (microfaults; Fig. 14F) and ductile deformation (folds, water escape structures; Fig. 14G, H).

Angular clasts found on the surface of ice-cored hummocks were probably transported into the lake basin either by sediment gravity flows caused by slumping of lateral moraine walls or as ice-rafted material (Benn & Owen 2002; Lukas *et al*. 2005). The presence of finer-grained sediment surrounding the clasts suggests they were emplaced subaqueously. Horizontally bedded sand (Sh; Fig. 14B) and rippled sand (Sr; Fig. 14E) are interpreted as the product of deposition from traction currents generated by underflows entering the lake (e.g. Eyles *et al*. 1987); structureless (Sm; Fig. 14B, C) and normally graded (Sg; Fig. 14G) sand facies record rapid deposition from sediment gravity flows and/or underflows. Deformed sand facies (Sd; Fig. 14F, G) are interpreted as the product of disturbance caused by underlying ice melt, topographic inversion, and slumping, as well as water escape caused by rapid sediment deposition (Eyles 1979; Miall 2010).

Alluvial fan (Logs 7–8; Fig. 16)

Coarse-grained facies. – Massive (structureless) sand and gravel facies (Sm, Gm; Fig. 14A) dominate sediments exposed in pits dug into the alluvial fans rimming the lake basin. Massive gravel facies contain subangular to subrounded clasts ranging in size from granules to boulders (5 mm to 30 cm; Fig. 15) and have a matrix of coarse-grained to silty sand.

These facies are interpreted as the product of rapid deposition from sediment gravity flows generated along the steep interior slopes of the lateral moraines enclosing the basin. Limited sorting of sediment grain sizes during down-slope transport has allowed the generation of distinct beds of gravel and sand; clasts are scattered throughout these deposits and their subangular to subrounded form suggests some abrasion has occurred during transport.

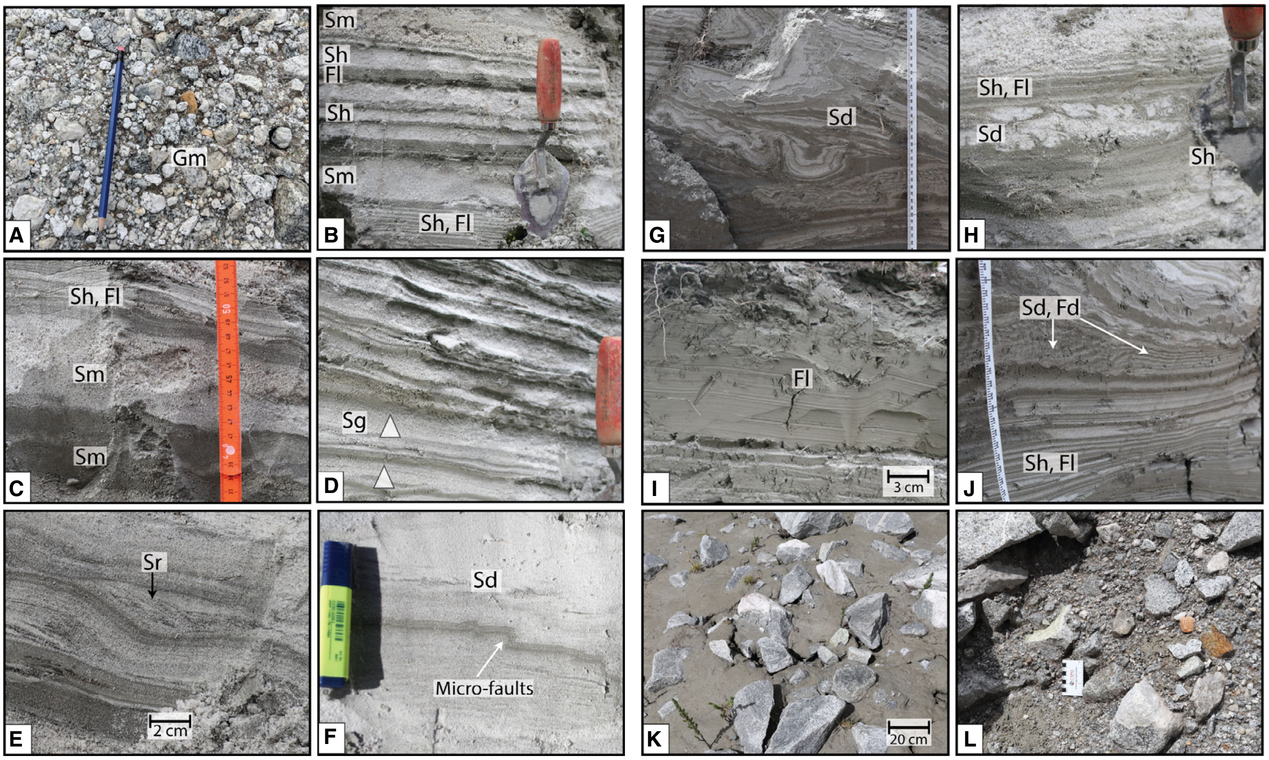

Fig. 14. Sediments within ice-cored hummocks. A. Massive gravel (Gm), subrounded to subangular clasts range from 5 mm to 2–3 cm. B. Interbedded medium sand (Sh, Sm) and laminated silts and muds (Fl). Trowel is 25 cm long. C. Two distinct beds of massive sand (Sm) overlain by interbedded sand and laminated fines (Sh, Fl). D. Normally graded sand beds (Sg) overlain by massive sand with thin silt interbeds. Normal grading symbol is shown in the white triangle. E. Medium-grained rippled sand unit (Sr; arrowed) within horizontally laminated sand. F. Micro-faults within medium-grained laminated sand. G. Deformed fine to coarse sand (Sd) and silty sand. H. Small dewatering structures within deformed sand (Sd). I. Finely laminated silt and clay (Fl). J. Deformed sand and deformed fines (Sd, Fd) showing a transition from severe to slight deformation from left to right of the image. Undeformed facies are shown beneath (Sh, Fl). K. Clasts on the surface of an ice-cored hummock. Clasts are angular to subangular; surrounding matrix is composed of silt to fine sand. L. Clast-rich surficial sediment comprising clasts in diameter from small granules (0.5 m) to clasts (~1 m).

Fine-grained facies. – Thin beds of massive fine sand and units of laminated silt are associated with coarser-grained sands and gravels in the alluvial fans (Fig. 16C, D). These fine-grained facies have similar characteristics to those described in ice-cored hummocks and a similar subaqueous origin is proposed. It is likely that water level changes in the lake have permitted periodic flooding of the distal margins of the alluvial fans.

Depositional history of Llaca Lake

The sediment exposures recorded here provide a series of 'snapshots' of depositional processes and environments that may exist in Llaca Lake at any one time. The majority of the exposures logged in ice-cored hummocks and fans extending into the lake show alternating beds of sand and fines (e.g. Sh, Fl; Fl, Sh; Fig. 15, Logs 1, 2, 3, 5) that record deposition under changing energy regimes related to variations in meltwater production (ablation), and/or rainfall events. Periods of relatively low sediment input to the lake are represented by units of laminated fine-grained sediment (Fl; Fl, Sh; Fig. 15, Log 6); sediment failure along the basin margins and/or rapid deposition caused by rapid melt and/or storm events are recorded by graded and deformed sand beds (Sg, Sd; Fig. 15, Logs 1, 2, 4, 6). It is important to note that depositional conditions that prevailed during accumulation of these sediments may also have been significantly influenced by frequent lake level changes and topographic adjustments caused by underlying ice melt. The dynamic distribution of sediment exposures in Llaca Lake creates complexity when attempting to generate an idealized stratigraphical model to describe its sedimentological characteristics. However, the description of depositional processes and products captured in this research provide a framework for the creation of a generalized facies model when data from additional moraine-dammed supraglacial lakes are available.

Landsystem zones within Llaca Lake

The geomorphological and sedimentological characteristics of Llaca Lake, a moraine-dammed supraglacial lake, are summarized in the schematic model shown in Fig. 17 and can be synthesized into three landsystem zones: Zone 1: distal portions of Llaca Lake and the

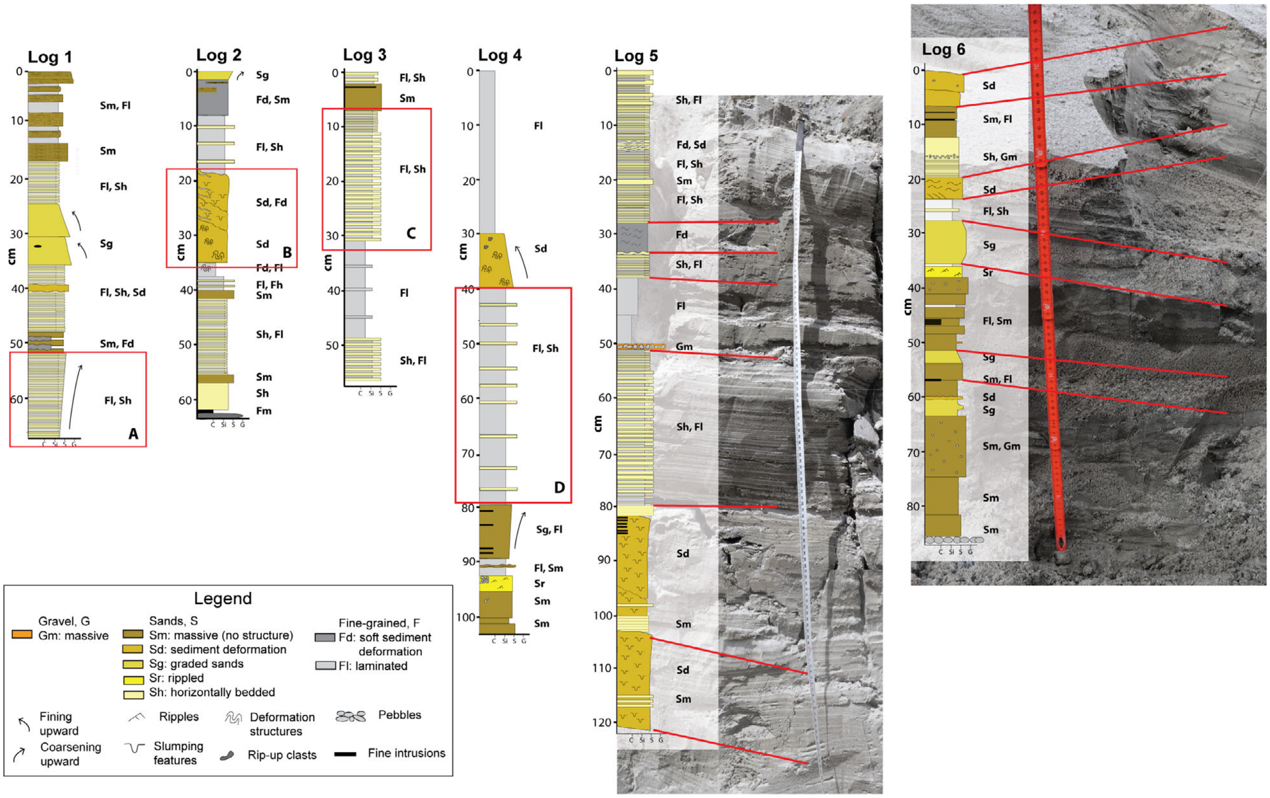

Fig. 15. Sedimentary logs recorded from exposures through ice-cored hummocks on Llaca Lake (see Fig. 6 for log locations) with areas of interest outlined by red boxes. A. Coarsening-upwards succession of interbedded sand and fine silt. B. Unit of deformed sand (Sd) and silt (Fd). C. Interbedded laminated silt and sand (Fl, Sh). D. Interbedded laminated silt and sand (Fl, Sh) with thick packages of fine silt (Fl) recording fluctuating energy regimes and/or sediment supply to the lake. Log 5 is dominated by interbedded laminated silt and sand (Fl, Sh) as well as deformation structures (Fd, Sd). Log 6 is dominated by sand facies (Sd, Sm, Sg, Sh, Sr) with some interbedded fines (Fl).

latero-frontal moraine; Zone 2: the central zone of ice-cored hummocks; and Zone 3: the active glacier margin. These zones are differentiated based on the spatial distribution of landforms, sediments, and active depositional processes.

Zone 1: Distal Llaca Lake and latero-frontal moraine

Zone 1 is bounded at its southern margin by the latero-frontal moraine that dams Llaca Lake. Sediment exposures through the moraine are limited and the moraine surface is partially covered by scrubby vegetation. While the internal sedimentary architecture of the moraine is unknown, examination of sediments exposed in similar moraines enclosing nearby lakes (e.g. Palcacocha; Bowman *et al.* 2018) suggests that it could contain a combination of clast- and matrix-supported massive diamicts with minor amounts of interbedded finer grained sediment (Fig. 8). The inner side of the moraine is prone to failure resulting in the transport of coarse-grained material into the lake (Fig. 11). The Zone 1 landsystem is also distinguished by the absence of ice-cored hummocks. Examination of historical images of the lake suggest that ice no longer underlies this distal region or is buried by deeper water; this is now the least dynamic zone within the moraine-dammed supraglacial lake landsystem.

Zone 2: Central zone of ice-cored hummocks

Zone 2 is characterized by ice-cored hummocks exposed above the water surface in Llaca Lake (Figs 4, 6, 9B). Sequential satellite imagery of this zone shows significant changes in the shape and size of these hummocks over time (Fig. 13) and suggests that the hummocks overlie progressively melting buried ice. Buried ice can be observed in debris-covered hummocks close to the modern ice margin (Fig. 9D) and it is possible that some of the buried ice is still connected to the main glacier. Although no systematic measurements of supraglacial debris thickness were made in this study, it has been estimated that it is generally in excess of 1 m and sufficient to insulate the ice beneath (Wigmore & Mark 2017). However, the uneven thickness of debris on the surface of the ice results in uneven amounts of insulation and causes differential melting rates (Nicholson *et al.* 2018). Differential melting creates a hummocky topography on the debris-covered ice surface and ultimately results in topographic inversion as supraglacial debris mixes with meltwater to create

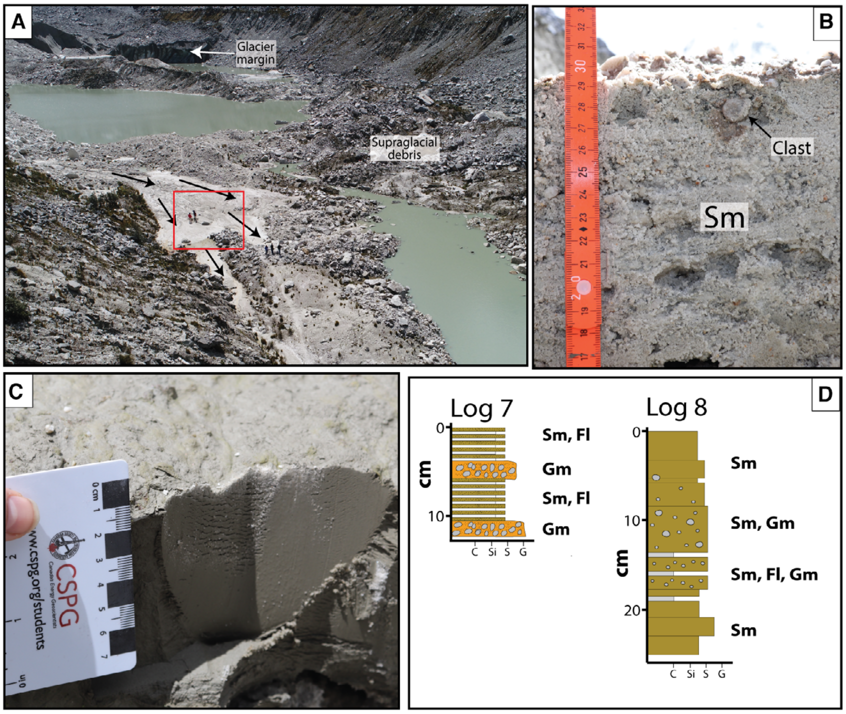

Fig. 16. Sedimentary facies within an alluvial fan. A. Location of alluvial fan on the margin of Llaca Lake. Flow paths on the surface of the fan are indicated by the black arrows. Red box shows location of excavated pits for photographs B, C and sedimentary logs shown in D. Figures in red box for scale. B. Massive sands with clasts on the surface of the fan. C. Fine-grained laminated silt and clay just below fan surface. D. Sedimentary logs recorded in two small pits dug into the alluvial fan showing areas dominated by laminated fines and gravels (Log 7) and massive sands and gravels (Log 8).

debrisflows that infill lows on the melting ice surface. Fine-grained sediment (dominantly silt and clay), introduced by inflowing meltwater from the glacier margin, accumulates as laminated deposits in areas covered by water. In addition to material that has been transported supraglacially and englacially, coarse-grained sediment is also introduced into the lake and onto the surface of the buried ice by alluvial fans and debrisflows from the steep inner slopes of the moraine (Fig. 9B, C). Alluvial fans contain a mixture of sand and gravel (Sm, Gm; Fig. 17, Log D) and rockfall debris is dominated by large (between 50 cm and 20 m diameter), angular blocks (Fig. 17, Log E).

Zone 3: Glacier margin

Zone 3 of the Llaca Lake landsystem incorporates the debris-covered terminus of Llaca Glacier (Fig. 9A) and includes proximal areas where stagnant ice is melting below a thick supraglacial cover producing hummocky topography, and steep-sided lateral moraines that contribute coarse angular debris to the ice surface and adjacent water bodies. The thick debris cover on Llaca Glacier (Fig. 9A) originates from rockfalls and avalanches from the steep bedrock valley walls. The terminus of the glacier is in contact with Llaca Lake and can be identified as an actively calving ice face (Fig. 10). Subglacial meltwater issues from the ice margin and transports coarse- and fine-grained sediment into the basin; subaqueous mass flow processes including turbidity currents and sediment gravity flows also transport sediment into the lake from areas proximal to the ice margin. Sediment failures from the debris-covered buried ice mass observed on the western margin of the lake body also contribute sediment to the lake (Fig. 9C).

The extent and location of Zone 3 are dynamic and change with the position of the active glacier terminus. As the glacier margin retreats, stagnant ice masses buried beneath the thick cover of supraglacial sediment and water of Llaca Lake slowly melt to produce an ice-cored hummocky topography similar to that present in Zone 2 (Figs 4, 10). The ice-proximal topography changes dramatically as ice retreats, buried ice melts, and the lake extends, creating a highly dynamic depositional environment (Figs 4, 10). Since 2017, two consistently enlarging water bodies have been observed in front of the glacier terminus (Figs 4, 10).

Discussion: Characteristics of a tropical moraine-dammed supraglacial lake landsystem

This study is the first to describe landform-sediment assemblages in a tropical moraine-dammed supraglacial lake in the Cordillera Blanca. The moraine-dammed supraglacial lake landsystem presented here for Llaca

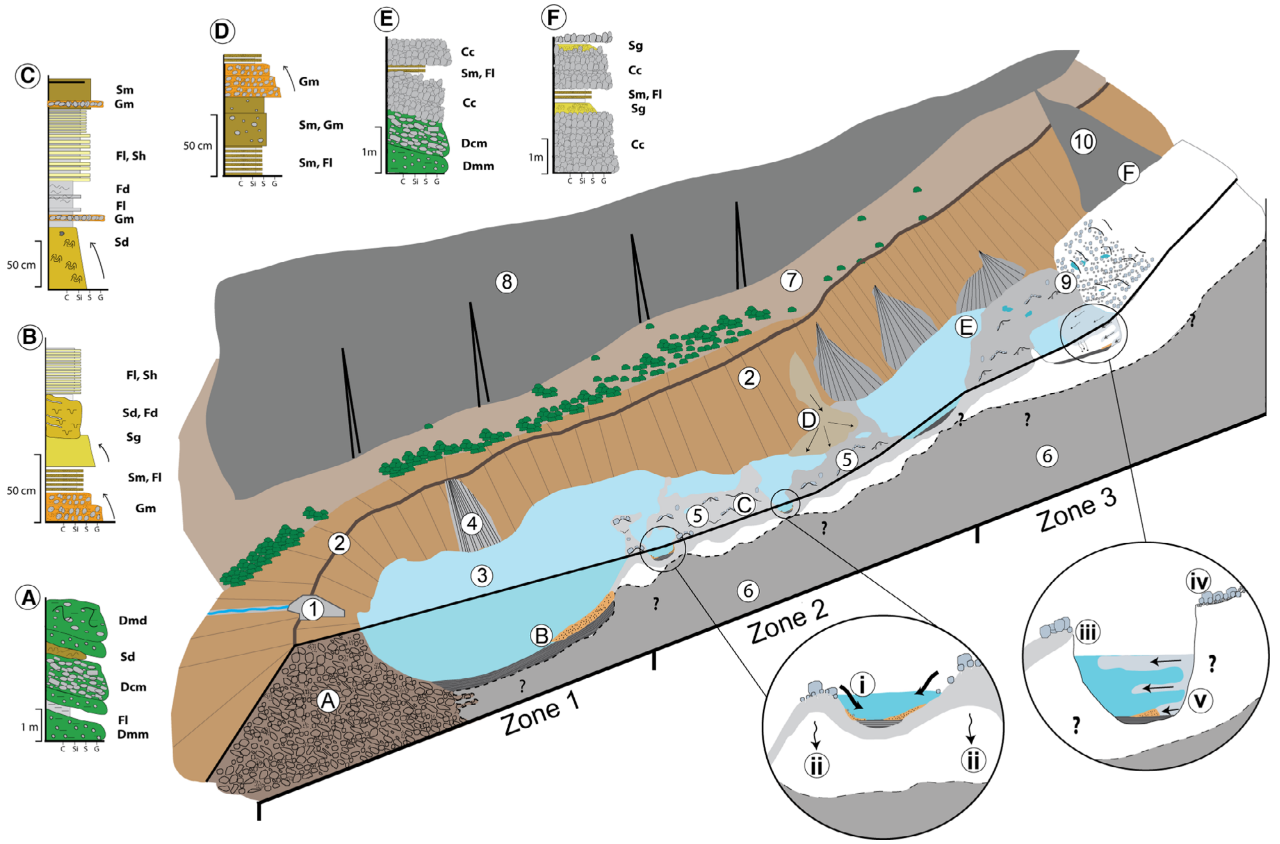

Fig. 17. Summary diagram to show the landsystem zones (Zones 1–3), landsystem elements (circled numbers 1–10), and idealized sedimentary logs (A–F) characteristic of Llaca Lake, a moraine-dammed supraglacial lake. Active processes shown by inset circles at lower right. Landsystem elements (circled numbers): 1 = outflow dam (Fig. 4) built in 1970 to monitor lake levels and water discharge; 2 = latero-frontal moraine that dams Llaca Lake; 3 = main water body of Llaca Lake with a maximum depth of ~20 m; 4 = moraine slope failures (Figs 9B–D, 11) that originate from the inside of the latero-frontal moraine; 5 = ice-cored hummocks; 6 = undetermined lake substrate – subglacial, supraglacial and slope-derived sediment overlying bedrock; 7 = outer moraine trough; 8 = valley walls composed of granodiorite; 9 = debris-covered glacier tongue covered by angular supraglacial debris ~1 m thick (Fig. 9B); 10 = rockfall and avalanche fans. Idealized sedimentary logs of selected environments (A–F): A = the latero-frontal moraine (Fig. 3) is likely to be composed of interbedded diamicts (Dmd, Dcm, Dmm) and fine-grained sediment (Fl, Sd); B = sediment found on the floor of Llaca Lake includes gravel (Gm) and sand (Sg, Sd, Sm) supplied by debrisflows, turbidites and/or slumping, and fine-grained sediment (Fl, Sh) from suspension; C = ice-cored hummocks contain sands carried into the lake by turbidites and/or underflows (Sh, Sm) and fines deposited from suspension (Fl). These facies show various amounts of soft sediment deformation (Sd, Fd); D = alluvial fans entering 46 the lake from the valley walls (Fig. 15) contain massive sands (Sm) and gravels bed (Gm) that fine upwards; E = moraine slope failures consist of stratified diamict and units of coarse angular debris with little to no fine matrix (Cc); F = rockfall and avalanche fans are characterized by crudely bedded, coarse-grained angular debris (Fig. 9A). Active processes (inset circles): i = slumping of debris from hummocks; ii = melting of buried ice beneath lacustrine/supraglacial sediment; iii = backwasting of buried ice (Fig. 9D); iv = active glacier terminus with supraglacial debris cover; v = underflows generated by cold, dense incoming meltwater.

Lake summarizes the active surface processes, sediments and resultant landforms that characterize this environment (Fig. 17). Previous studies of glaciated valley landsystems have focused on those in cold temperate regions (i.e. Boulton & Eyles 1979; Eyles 1979, 1983a, b; Kirkbride & Spedding 1996; Benn & Owen 2002; Spedding & Evans 2002; Benn *et al*. 2003). Many of the factors noted to control landform development in temperate glaciated valleys (such as topography, debris supply to the glacier surface, and efficiency of sediment transport from glacier to ice-proximal environments, e.g. Benn *et al*. 2003) also operate at Llaca Lake and Llaca Glacier, allowing similar landsystem elements to develop. However, the deglaciating valleys of the Cordillera Blanca are very steep and narrow, focussing mass movement and fluvial processes, which efficiently rework and redistribute sediment along the valley floors. As a result, the record of past glacial activity is sparse and poorly preserved making palaeoenvironmental reconstruction of deglaciation processes in these valleys extremely difficult. Lake basins such as Llaca Lake are therefore important repositories of the sedimentary record of recent glacial recession and palaeoenvironmental change. Unfortunately, the presence of buried ice within Llaca Lake and the development of an irregular lake floor topography created by ice-cored hummocks significantly affect the distribution of fine- (Fl) and coarse-grained sediments (Sg, Sr, Sd) in the lake basin. Topographic inversion, caused by the uneven melting of buried ice, not only creates water-filled topographic lows that form sediment depocentres, but also causes extensive mixing and deformation of accumulating sediment. The ice-cored hummocks in Llaca Lake are constantly changing in size and distribution (Figs 5, 12, 13) and those visible today will likely be submerged as buried ice continues to melt. It is difficult to predict the characteristics of the sediment stratigraphy that will eventually be preserved within the Llaca Lake basin other than to say there will be interbedding of both coarse- and fine-grained sediments, which will be extensively deformed in places. However, it is important to gain an understanding of the processes responsible for the delivery, accumulation and preservation of these sediments in order to design appropriate coring and sampling programmes for future palaeoenvironmental investigations.

The landsystem characteristics described here at Llaca Lake are very similar to those described at enlarging glacial lakes formed at the margins of retreating debris-covered glaciers in high-altitude regions of the Himalaya (Benn *et al.* 2012). Examination of numerous retreating Himalayan glacier margins has allowed the identification of three distinct process regimes resulting from progressive glacier ablation including an initial regime of active ice flow with ice filling the lake basin, a second regime characterized by stagnant downwasting ice, and a third regime in which a rapidly expanding lake forms behind a moraine dam (Benn *et al.* 2012). Llaca Lake appears to have characteristics that place it in the transition zone between the second and third Himalayan regimes. This is considered to be a particularly hazardous position, given current climatic conditions that allow enhanced ablation of glacier ice and growth of the impounded lake, enhancing the potential for GLOF generation (Benn *et al.* 2012). Since 2005, the surface area of open water in Lake Llaca has increased at a rapid rate (Fig. 5). The progressive melting of buried ice in the Llaca Lake basin will increase the volume of water that can be contained within the basin, ultimately increasing the risk and impact of a future GLOF (Benn *et al.* 2012). It will be important to continuously monitor ice melt and lake level fluctuations over the coming years as Llaca Glacier continues to melt.

Conclusions

Glaciers in the Cordillera Blanca, Perú have been severely impacted by recent climate change allowing the number and size of ice-marginal glacial lakes to increase substantially. Unfortunately, little is known about the processes operating within these growing lakes, their stability, or their palaeoenvironmental signature. This study presents a detailed geomorphological and sedimentological assessment of Llaca Lake, a moraine-dammed tropical supraglacial lake in the Cordillera Blanca and documents the dominant landscape features and sediment types that characterize the environment. The use of UAV-derived photogrammetric orthomosaics and DEMs, in addition to field-based data and remotely sensed aerial imagery, has allowed high-resolution analysis of the landforms and surface sediments in the lake and the delineation of landform elements. Modern depositional processes in the lake are dominated by factors controlling sediment input and distribution from steep valley walls and from meltwater streams and debris-covered melting ice. Coarse-grained material has accumulated around the lake margins to form landform elements such as the impounding latero-frontal moraine, and rockfall and alluvial fans (Fig. 17). Extensive areas of ice-cored hummocks expose both coarse- and fine-grained, often deformed, sediment previously deposited by debrisflows, turbidites/underflows, variable traction currents, and ice-rafting in the lake basin (Fig. 17). The distribution of ice-cored hummocks in the lake changes substantially over time as underlying ice melts and sediment is redistributed, creating dynamic and constantly changing depositional conditions. These temporal changes in depositional conditions also allow Llaca Lake to be subdivided into three spatially distinct landsystem zones comprising the latero-frontal moraine and ice-distal open water areas (Zone 1), the central area of the lake dominated by ice-cored hummocks (Zone 2) and the ice-proximal area adjacent to the active glacier margin (Zone 3). The boundaries between each of these zones constantly change as depositional environments adjust to glacier margin retreat, buried ice melt, and water level changes. The geomorphological and sedimentological signature of such a dynamic environment is therefore complex and the Llaca Lake landsystem presented here should therefore be considered as a snapshot in time.

There is a growing demand to understand the sedimentary records of glacial lakes in the Cordillera Blanca to facilitate understanding of climatic change in the Southern Hemisphere during the Holocene (Stansell *et al.* 2015; Mark *et al.* 2017). Analysis of fine-grained lake sediments, including sedimentological, micropalaeontological and geochemical analyses (e.g. Last & Vance 2002; Haberzettl *et al.* 2007; Thomas & Briner 2009; Larsen *et al.* 2011; Stansell *et al.* 2013, 2014) can provide valuable palaeoclimatic information. However, understanding the nature of the modern landsystem elements, their changing spatial distribution, and the sedimentary record of these dynamic glacial lakes, is also necessary. Better understanding of the long-term evolution of these lakes and their water storage capacity is also essential for local communities that rely on them for water supply (Viviroli *et al.* 2011). Diminishing water supply as glaciers recede is not an issue restricted to the Cordillera Blanca but is a real threat in many high-altitude areas across the globe.

Acknowledgements. – This research was funded by a Global Science Initiatives grant from the Faculty of Science at McMaster University, an NSERC Discovery Grant to CHE (RGPIN-2019-06568) and an NSERC CGS D Doctoral Award. Logistical support for fieldwork was provided by INAIGEM. We would like to thank Dr Simon Cook and an anonymous reviewer for their helpful comments and Jan A. Piotrowski for his editorial support.

Author contributions. – All authors were involved in the collection of field data. RANP arranged fieldwork, analysed imagery, created figures (including landsystem element map), and prepared the manuscript with contributions from all authors. CHE helped design the study and interpret sedimentological data. REL was responsible for UAV flying and interpretation of UAV data. LDR arranged field logistics and JCM helped interpret geomorphological data. The authors declare that they have no conflict of interest.

References

Autoridad Nacional del Agua (ANA) 2020: *Lagunas - Reservas de agua dulce en Áncash: resultados de estudios de batimetría en 38 lagunas glaciares. Huaraz, Perú.* 94 pp. Autoridad Nacional del Agua, Perú.

Barnett, T. P., Adam, J. C. & Lettenmaier, D. P. 2005: Potential impacts of a warming climate on water availability in snow-dominated regions. *Nature 438*, 303–309.

Barr, I. D. & Lovell, H. 2014: A review of topographic controls of moraine distribution. *Geomorphology 226*, 44–64.

Benn, D. I. & Owen, L. A. 2002: Himalayan glacial sedimentary environments: a framework for reconstructing and dating the former extent of glaciers in high mountains. *Quaternary International 97–98*, 3–25.

Benn, D. I., Bolch, T., Hands, K., Gulley, J., Luckman, A., Nicholson, L. I., Quincey, D., Thompson, S., Toumi, R. & Wiserman, S. 2012: Response of debris-covered glaciers in the Mount Everest region to recent warming, and implications for outburst flood hazards. *Earth-Science Reviews 114*, 156–174.

Benn, D. I., Kirkbride, M. P., Owen, L. A. & Brazier, V. 2003: Glaciated valley landsystems. *In* Evans, D. J. A. (ed.): *Glacial Landsystems*, 372–406. Hodder Arnold, London.

Bennett, G. L., Evans, D. J. A., Carbonneau, P. & Twigg, D. R. 2010: Evolution of a debris-charged glacier landsystem, Kvíárjökull, Iceland. *Journal of Maps 6*, 40–67.

Boulton, G. S. & Eyles, N. 1979: Sedimentation by valley glaciers; a model and genetic classification. *In* Schlüchter, C. (ed.): *Proceedings of an INQUA Symposium on Genesis and Lithology of Quaternary Deposits*, 11–24. A.A. Balkema, Rotterdam.

Bowman, D., Eyles, C. H., Narro-Pérez, R. & Vargas, R. 2018: Sedimentology and structure of the Lake Palcacocha Laterofrontal moraine complex in the Cordillera Blanca, Peru. *Revista de Glaciaers y Ecosistemas de Montaña 5*, 27–42.

Bury, J., Mark, B. G., Carey, M., Young, K. R., McKenzie, J. M., Baraer, M., French, A. & Polk, M. H. 2013: New geographies of water and climate change in Peru: coupled natural and social transformations in the Santa River watershed. *Annals of the Association of American Geographers 103*, 363–374.

Carey, M. 2005: Living and dying with glaciers: people's historical vulnerability to avalanches and outburst floods in Peru. *Global and Planetary Change 47*, 122–134.

Carey, M. 2010: *In the Shadow of Melting Glaciers: Climate Change and Andean Society.* 273 pp. Oxford University Press, New York.

Carey, M., Huggel, C., Bury, J., Portocarrero, C. & Haeberli, W. 2012: An integrated socio-environmental framework for glacier hazard management and climate change adaptation: lessons from Lake 513, Cordillera Blanca, Peru. *Climatic Change 112*, 733–767.

Chandler, B. M. P., Evans, D. J. A., Chandler, S. J. P., Ewertowski, M. W., Lovell, H., Roberts, D. H., Schaefer, M. & Tomczyk, A. M. 2020: The glacial landsystem of Fjallsjökull, Iceland: spatial and temporal evolution of process-form regimes at an active temperate glacier. *Geomorphology 361*, 107192, https://doi.org/10.1016/j.geomorph.2020.107192.

Chikita, K., Jha, J. & Yamada, T. 2001: Sedimentary effects on the expansion of a Himalayan supraglacial lake. *Global and Planetary Change 28*, 23–34.

Clapperton, C. M. 1972: The Pleistocene moraine stages of west-Central Peru. *Journal of Glaciology 11*, 255–263.

Cobbing, E. J., Pitcher, W. S., Wilson, J. J., Baldock, J. W., Taylor, W. P., McCourt, W. J. & Snelling, N. J. 1981: *Estudio geológico de la Cordillera Occidental del norte del Perú.* 252 pp. Institute Geologico Minero y Metalurgico (INGEMMET), Peru.

Concha, J. F. 1951: *Origen de las lagunas.* 4 pp. Corporación Peruana del Santa, Huaraz, Perú.

Cook, S. J. & Quincey, D. J. 2015: Estimating the volume of Alpine glacial lakes. *Earth Surface Dynamics 3*, 559–575.

Deverchère, J., Dorbath, C. & Dorbath, L. 1989: Extension related to a high topography: results from a microearthquake survey in the Andes of Peru and tectonic implications. *Geophysical Journal International 98*, 281–292.

Ely, J. C., Graham, C., Barr, I. D., Rea, B. R., Spagnolo, M. & Evans, J. 2017: Using UAV acquired photography and structure from motion techniques for studying glacier landforms: application to the glacial flutes at Isfallsglaciären. *Earth Surface Processes and Landforms 42*, 877–888.

Emmer, A. & Vilímek, V. 2013: Review article: lake and breach hazard assessment for moraine-dammed lakes: an example from the Cordillera Blanca (Peru). *Natural Hazards and Earth System Sciences 13*, 1551–1565.

Emmer, A., Harrison, S., Mergili, M., Allen, S., Frey, H. & Huggel, C. 2020: 70 years of lake evolution and glacial lake outburst floods in the Cordillera Blanca (Peru) and implications for the future. *Geomorphology 365*, 107178, https://doi.org/10.1016/j.geomorph.2020.107178.

Emmer, A., Klimeŝ, J., Mergili, M., Vilímek, V. & Cochachin, A. 2016: 882 lakes of the Cordillera Blanca: an inventory, classification, evolution and assessment of susceptibility to outburst floods. *Catena 147*, 269–279.

Emmer, A., Vilímek, V. & Zapata, M. L. 2018: Hazard mitigation of glacial lake outburst floods in the Cordillera Blanca (Peru): the effectiveness of remedial works. *Journal of Flood Risk Management 11*, S489–S501.

Emmer, A., Wood, J. L., Cook, S. J., Harrison, S., Wilson, R., Diaz-Moreno, A., Reynold, J. M., Torres, J. C., Yarleque, C., Mergili, M., Jara, H. W., Bennett, G., Caballero, A., Glasser, N. F., Malgarejo, E., Riveros, C., Shannon, S., Turpo, E., Tinoco, T., Torres, L., Garay, D., Villafane, H., Garrido, H., Martinez, C., Apaza, N., Arajuo, J. & Poma, C. 2022: 160 glacial lake outburst flood (GLOFs) across tropical Andes since the Little Ice Age. *Global and Planetary Change 208*, 103722, https://doi.org/10.1016/j.gloplacha.2021.103722.

ESRI 2019: *DigitalGlobe (WV02) image captured on Aug 2, 2017 as shown in the 2019-12-12 version of the World Imagery map.* Available at: https://livingatlas.arcgis.com/wayback/#active=4756&ext=-77.45567,-9.44392,-77.42198,-9.42319 (accessed 11.02.2020).

Evans, D. J. A. 2003: Introduction to glacial landsystems. *In* Evans, D. J. A. (ed.): *Glacial Landsystems*, 1–11. Hodder Arnold, London.

Evans, S. G. & Clague, J. J. 1994: Recent climatic change and catastrophic geomorphic processes in mountain environments. *Geomorphology 10*, 107–128.

Evans, D. J. A., Ewertowski, M. & Orton, C. 2016: Fláajökull (north lobe), Iceland: active temperate piedmont lobe glacial landsystem. *Journal of Maps 12*, 777–789.

Evans, D. J. A., Ewertowski, M. & Orton, C. 2017: The glaciated valley landsystem of Morsárjökull, Southeast Iceland. *Journal of Maps 13*, 909–920.

Evans, D. J. A., Lemmen, D. S. & Rea, B. R. 1999: Glacial landsystems of the southwest Laurentide ice sheet: modern Icelandic analogues. *Journal of Quaternary Science 14*, 673–691.

Evans, D. J. A., Shulmeister, J. & Hyatt, O. 2010: Sedimentology of latero-frontal moraines and fans on the west coast of South Island, New Zealand. *Quaternary Science Reviews 29*, 3790–3811.

Eyles, N. 1979: Facies of supraglacial sedimentation on Icelandic and Alpine temperate glaciers. *Canadian Journal of Earth Sciences 16*, 1341–1361.

Eyles, N. 1983a: Glacial geology: a landsystems approach. *In* Eyles, N. (ed.): *Glacial Geology: An Introduction for Engineers and Earth Scientists*, 1–18. Pergamon Press, Toronto.

Eyles, N. 1983b: The glaciated valley landsystem. *In* Eyles, N. (ed.): *Glacial Geology*, 91–110. Pergamon Press, Toronto.

Eyles, N. 1993: Earth's glacial record and its tectonic setting. *Earth-Science Reviews 35*, 1–248.

Eyles, N. & Clark, B. M. 1988: Storm-influenced deltas and ice scouring in a late Pleistocene glacial lake. *Geological Society of America Bulletin 100*, 793–809.

Eyles, C. H. & Eyles, N. 2010: Glacial deposits. *In* James, N. P. & Dalrymple, R. W. (eds.): *Facies Model 4*, 73–104. Geological Society of Canada, St. John's Newfoundland & Labrador.

Eyles, N., Clark, B. M. & Clague, J. J. 1987: Coarse-grained sediment gravity flow facies in a large supraglacial lake. *Sedimentology 34*, 193–216.

Eyles, N., Eyles, C. H. & Miall, A. D. 1983: Lithofacies types and vertical profile models; an alternative approach to the description and environmental interpretation of glacial diamict and diamictite sequence. *Sedimentology 30*, 393–410.

Fitzsimons, S. J. 2003: Ice-marginal terrestrial landsystems: polar-continental glacier margins. *In* Evans, D. J. A. (ed.): *Glacial Landsystems*, 89–110. Hodder Arnold, London.

Gauthier, D., Wood, D. F. & Hutchinson, D. J. 2015: *Natural geologic controls on rockfall hazard and mitigation on the Niagara escarpment, King's highway 403 at Hamilton, ON, Canada*. In 66th Highway Geology Symposium, 520–534. Sturbridge, Massachusetts. Available at: http://www.highwaygeologysymposium.org/wp-content/uploads/66_HGS-OPT.pdf.

Georges, C. 2004: 20th-century glacier fluctuations in the tropical Cordillera Blanca, Perú. *Arctic, Antarctic, and Alpine Research 36*, 100–107.

Giovanni, M. K., Horton, B. K., Garzione, C. N., McNulty, B. & Grove, M. 2010: Extensional basin evolution in the Cordillera Blanca, Peru: stratigraphic and isotopic records of detachment faulting and orogenic collapse in the Andean hinterland. *Tectonics 29*, TC6007, https://doi.org/10.1029/2010TC002666.

Glasser, N. F. & Hambrey, M. J. 2003: Ice-marginal terrestrial landsystems: Svalbard polythermal glaciers. *In* Evans, D. J. A. (ed.): *Glacial Landsystems*, 65–88. Arnold Hodder, London.

Google Earth V. 7.3.4.8248 June 1, 2005: Llaca Lake, Cordillera Blanca, Perú. 9°26′0.88″ S, 77°26′38.55″ W. Eye alt. 8.30km. Maxar Technologies. Available at: www.earth.google.com (accessed 28.04.2021).

Google Earth V. 7.3.4.8248 July 12, 2011: Llaca Lake, Cordillera Blanca, Perú. 9°26′0.88″ S, 77°26′38.55″ W. Eye alt. 8.30km. Maxar Technologies. Available at: www.earth.google.com (accessed 28.04.2021).

Google Earth V. 7.3.4.8248 August 19, 2013: Llaca Lake, Cordillera Blanca, Perú. 9°26′0.88″ S, 77°26′38.55″ W. Eye alt. 8.30km. CNES/Airbus. Available at: www.earth.google.com (accessed 28.04.2021).

Google Earth V. 7.3.4.8248 May 29, 2016: Llaca Lake, Cordillera Blanca, Perú. 9°26′0.88″ S, 77°26′38.55″ W. Eye alt. 8.30km. CNES/Airbus. Available at: www.earth.google.com (accessed 28.04.2021).

Google Earth V. 7.3.4.8248 August 2, 2017: Llaca Lake, Cordillera Blanca, Perú. 9°26′0.88″ S, 77°26′38.55″ W. Eye alt. 8.30km. Maxar Technologies. Available at: www.earth.google.com (accessed 28.04.2021).

Google Earth V. 7.3.4.8248 June 21, 2019: Llaca Lake, Cordillera Blanca, Perú. 9°26′0.88″ S, 77°26′38.55″ W. Eye alt. 8.30km. CNES/Airbus. Available at: www.earth.google.com (accessed 28.04.2021).

Haberzettl, T., Coberlla, H., Fey, M., Janssen, S., Lucke, A., Mayr, C., Ohlendorf, C., Schäbitz, F., Schleser, G. H., Wille, M., Wulf, S. & Zolitschka, B. 2007: Lateglacial and Holocene wet-dry cycles in southern Patagonia: chronology, sedimentology and geochemistry of a lacustrine record from Laguna Potrok Aike, Argentina. *The Holocene 17*, 297–310.

Harrison, S., Kargel, J. S., Huggel, C., Reynolds, J., Shugar, D. H., Betts, R. A., Emmer, A., Glasser, N., Haritashya, U. K., Klimes, J., Reinhardt, L., Shaub, Y., Wiltshire, A., Regmi, D. & Vilímek, V. 2018: Climate change and the global pattern of moraine-dammed glacial lake outburst floods. *The Cryosphere 12*, 1195–1209.

Hock, R., Rasul, G., Adler, C., Cáceres, B., Gruber, S., Hirabayashi, Y., Jackson, M., Kääb, A., Kang, S., Kutuzov, S., Milner, A., Molau, U., Morin, S., Orlove, B. & Stelzer, H. 2019: High mountain areas. *In* Pörtner, H.-O., Roberts, D. C., Masson-Delmotte, V., Zhai, P., Tignor, M., Poloczanska, E., Mintenbeck, K., Alegría, A., Nicolai, M., Okem, A., Petzold, J., Rama, B. & Weyer, N. M. (eds.): *IPCC Special Report Ocean and Cryosphere in a Changing Climate*, 131–202. Cambridge University Press, New York.

Hubbard, B., Heald, A., Reynold, J. M., Quincey, D., Richardson, S. D., Zapata Luyo, M., Santillan Portilla, N. & Hambrey, M. J. 2005: Impact of a rock avalanche on a moraine-dammed proglacial lake: Laguna Safuna Alta, Cordillera Blanca, Peru. *Earth Surface Processes and Landforms 30*, 1251–1264.

Huggel, C., Carey, M., Clague, J. J. & Kääb, A. 2015: Introduction: human-environment dynamics in the high-mountain cryosphere. *In* Huggel, C., Carey, M., Clague, J. J. & Kääb, A. (eds.): *The High-Mountain Cryosphere - Environmental Changes and Human Risks*, 1–6. Cambridge University Press, New York.

Humlum, O. 1978: Genesis of layered moraines: implications for palaeoclimatology and lichenometry. *Geografisk Tidsskrift-Danish Journal of Geography 77*, 65–72.

Instituto Nacional De Investigación en Glaciares y Ecosistemas de Montaña (INAIGEM) 2018: *Inventario Nacional de Glaciares: Las Cordilleras Glaciares del Peru*. 348 pp. Instituto Nacional de Investigación en Glaciares y Ecosistemas de Montaña Biblioteca y Publicaciones, Huaraz, Peru.

Irvine-Flynn, T. D. L., Porter, P. R., Rowan, A. V., Quincey, D. J., Gibson, M. J., Bridge, J. W., Watson, C. S., Hubbard, A. & Glasser, N. F. 2017: Supraglacial ponds regulate runoff from Himalayan debris-covered glaciers. *Geophysical Research Letters 44*, 11894–11904.

Iturrizaga, L. 2014: Glacial and glacially conditioned lake types in the Cordillera Blanca, Peru: a spatiotemporal conceptual approach. *Progress in Physical Geography 38*, 602–636.

Kaser, G. 2001: Glacier-climate interaction at low latitudes. *Journal of Glaciology 47*, 195–204.

Kershaw, J. A., Clague, J. J. & Evans, S. G. 2005: Geomorphic and sedimentological signature of a two-phase outburst flood from moraine-dammed Queen Bess Lake, British Columbia, Canada. *Earth Surface Processes and Landforms 30*, 1–25.

Kirkbride, M. & Spedding, N. 1996: The influence of englacial drainage on sediment-transport pathways and till texture of temperate valley glaciers. *Annals of Glaciology 22*, 160–166.

Klimeš, J., Benešová, M., Vilímek, V., Bouška, P. & Cochachin Rapre, A. 2014: The reconstruction of a glacial lake outburst flood using HEC-RAS and its significance for future hazard assessments: an example from Lake 513 in the Cordillera Blanca, Peru. *Natural Hazards 71*, 1617–1638.

Klimeš, J., Vilímek, V. & Omelka, M. 2009: Implications of geomorphological research for recent and prehistoric avalanches and related hazards at Huascaran, Peru. *Natural Hazards 50*, 193–209.

Larsen, D. J., Miller, G. H., Geirsdóttir, Á. & Thordarson, T. 2011: A 3000-year varved record of glacier activity and climate change from the proglacial lake Hvítárvatn, Iceland. *Quaternary Science Reviews 30*, 2715–2731.

Last, W. M. & Vance, R. E. 2002: The Holocene history of Oro Lake, one of the western Canada's longest continuous lacustrine records. *Sedimentary Geology 148*, 161–184.

Lee, E., Carrivick, J. L., Quincy, D. J., Cook, S. J., James, W. H. M. & Brown, L. E. 2021: Accelerated mass loss of Himalayan glaciers since the little ice age. *Nature Scientific Reports 11*, 24284, https://doi.org/10.1038/s41598-021-03805-8.

Lee, R. E., Maclachlan, J. C. & Eyles, C. H. 2018: Landsystems of Morsárjökull, Skaftafellsjökull and Svínafellsjökull, outlet glaciers of the Vatnjökull Ice Cap, Iceland. *Boreas 47*, 1199–1217.

Lukas, S. 2008: A test of the englacial thrusting hypothesis of "hummocky" moraine formation: case studies from the northwest Highlands, Scotland. *Boreas 34*, 287–307.

Lukas, S. 2012: Processes of annual moraine formation at a temperate alpine valley glacier: insights into glacier dynamics and climate controls. *Boreas 41*, 463–480.

Lukas, S., Nicholson, L. I., Ross, F. H. & Humlum, O. 2005: Formation, Meltout processes and landscape alteration of high-Arctic ice-cored moraines—examples from Nordenskiold Land, Central Spitsbergen. *Polar Geography 29*, 157–187.

Lynch, B. D. 2012: Vulnerabilities, competition and rights in a context of climate change toward equitable water governance in Peru's Rio Santa Valley. *Global Environmental Change 22*, 364–373.

Małecki, J., Lovell, H., Ewertowski, W., Górski, Ł., Kurczaba, T., Latos, B., Miara, M., Piniarska, D., Płoncieniczak, J., Sowada, T., Spiralski, M., Warczachowska, A. & Rabatel, A. 2018: The glacial landsystem of a tropical glacier: Charquini Sur, Bolivian Andes. *Earth Surface Processes and Landforms 43*, 2584–2602.

Margirier, A., Audin, L., Robert, X., Herman, F., Ganne, J. & Schwartz, S. 2016: Time and mode of exhumation of the Cordillera Blanca batholith (Peruvian Andes). *Journal of Geographical Research: Solid Earth 121*, 6235–6249.

Margirier, A., Braun, J., Robert, X. & Audin, L. 2018: Role of erosion and isostasy in the Cordillera Blanca uplift: insights from landscape evolution modeling (northern Peru, Andes). *Tectonophysics 728–729*, 119–129.

Mark, B. G. & Seltzer, G. O. 2005: Evaluation of recent glacier recession in the Cordillera Blanca, Peru (AD 1962–1999): spatial distribution of mass loss and climatic forcing. *Quaternary Science Reviews 24*, 2265–2280.

Mark, B., Stansell, N. & Zeballos, G. 2017: The last deglaciation of Peru and Bolivia. *Cuadernos de Investigación Geográfica 43*, 591–628.

Mark, B. G., Bury, J., McKenzie, J. M., French, A. & Baraer, M. 2010: Climate change and tropical Andean glacier recession: evaluating hydrologic changes and livelihood vulnerability in the Cordillera Blanca, Peru. *Annals of the Association of American Geographers 100*, 794–805.

McNulty, B. & Farber, D. 2002: Active detachment faulting above the Peruvian flat slab. *Geology 30*, 567–570.

Mergili, M., Shiva, P. P., Emmer, A., Fischer, J.-T., Cochachin, A. & Frey, H. 2020: Reconstruction of the 1941 GLOF process chain at Lake Palcacocha (Cordillera Blanca, Peru). *Hydrology and Earth System Sciences 22*, 93–114.

Miall, A. 2010: Alluvial deposits. *In* James, N. P. & Dalrymple, R. W. (eds.): *Facies Model 4*, 105–138. Geological Association of Canada, St. John's.

Miles, E. S., Watson, C. S., Brun, F., Berthier, E., Esteves, M., Quince, D. J., Miles, K. E., Hubbard, B. & Wagnon, P. 2018: Glacial and geomorphic effects of a supraglacial lake drainage and outburst event, Everest region, Nepal Himalaya. *The Cryosphere 12*, 3891–3905.

Muñoz, R., Huggle, C., Frey, H., Cochachin, A. & Haeberli, W. 2020: Glacial lake depth and volume estimation based on a large bathymetric dataset from the Cordillera Blanca, Peru. *Earth Surface Processes and Landforms 45*, 1510–1527.

Nicholson, L. I., McCarthy, M., Pritchard, H. D. & Willis, I. 2018: Supraglacial debris thickness variability: impact on ablation and relation to terrain properties. *The Cryosphere 12*, 3719–3734.

Owen, L. A. & Derbyshire, E. 1989: The Karakoram glacial depositional system. *Zeitschrift für Geomorphologie 76*, 33–73.

Owen, L. A., Robinson, R., Benn, D. I., Finkel, R. C., Davis, N. K., Yi, C., Putkonen, J., Li, D. & Murray, A. S. 2009: Quaternary glaciation of Mount Everest. *Quaternary Science Reviews 28*, 1412–1433.

Portocarrero, C. A. 2014: *The Glacial Lake Handbook: Reducing Risk From Dangerous Glacial Lakes in the Cordillera Blanca, Peru*. 80 pp. United States Agency for International Development, Global Climate Change Office, Climate Change Resilient Development Project, Washington DC.

Rabatel, A., Francou, B., Soruco, A., Gomez, J., Cáceres, B., Ceballos, J. L., Basantes, R., Vuille, M., Sicart, J.-E., Huggel, C., Scheel, M., Lejeune, Y., Arnoud, Y., Collet, M., Condom, T., Consoli, G., Favier, V., Jomelli, V., Galarrage, R., Ginot, P., Maisincho, L., Mendoza, J., Ménégoz, M., Ramirez, E., Ribstein, P., Suarez, W., Villacis, M. & Wagnon, P. 2013: Current state of glaciers in the tropical Andes: a multi-century perspective on glacier evolution and climate change. *The Cryosphere 7*, 81–102.

Rangwala, I., Pepin, N., Vuille, M. & Miller, J. 2015: Influence of climate variability and large-scale circulation on the mountain cryosphere. *In* Huggel, C., Carey, M., Clague, J. J. & Kääb, A. (eds.): *The High-Mountain Cryosphere - Environmental Changes and Human Risks*, 9–27. Cambridge University Press, New York.

Rodbell, D. T. 1992: Lichenometric and radiocarbon dating of Holocene glaciation, Cordillera Blanca, Perú. *The Holocene 2*, 19–29.

Schauwecker, S., Roher, M., Acuña, D., Cochachin, A., Dávila, L., Frey, H., Giráldez, C., Gómez, J., Huggel, C., Jacques-Coper, M., Loarte, E., Salzmann, N. & Vuille, M. 2014: Climate trends and glacier retreat in the Cordillera Blanca, Peru, revisited. *Global and Planetary Change 119*, 85–97.

Schneider, D., Huggel, C., Cochachin, A., Guillén, S. & García, J. 2014: Mapping hazards from glacier Lake outburst floods based on modelling of process cascades at Lake 513, Carhuaz, Peru. *Advances in Geosciences 35*, 145–155.

Schomacker, A., Benediktsson, Í. Ö. & Ingólfsson, Ó. 2014: The Eyjabakkajökull glacial landsystem, Iceland: geomorphic impact of multiple surges. *Geomorphology 218*, 98–107.

Schwartz, D. P. 1988: Paleoseismicity and neotectonics of the Cordillera Blanca fault zone, northern Peruvian Andes. *Journal of Geophysical Research: Solid Earth 93*, 4712–4730.

Shugar, D. H., Burr, A., Haritashya, U. K., Kargel, J. S., Watson, C. S., Kennedy, M. C., Bevington, A. R., Betts, R. A., Harrison, S. & Strattman, K. 2020: Rapid worldwide growth of glacial lakes since 1990. *Nature Climate Change 10*, 939–945.

Sigurðardóttir, M. 2013: *The sedimentology and formation of the Gígjökull and Kvíárjökull latero-frontal moraines, Iceland*. M.Sc. thesis, University of Iceland, 89 pp.

Silverio, W. & Jaquet, J. M. 2017: Evaluating glacier fluctuations in Cordillera Blanca (Peru) by remote sensing between 1987 & 2016 in the context of ENSO. *Archives des Sciences 69*, 145–162.

Smith, J. A., Seltzer, G. O., Farber, D. L., Rodbell, D. T. & Finkel, R. C. 2005: Early local last glacial maximum in the tropical Andes. *Science 308*, 678–681.

Somos-Valenzuela, M. A., Chisolm, R. E., Rivas, D. S., Portocarrero, C. & McKinney, D. C. 2016: Modeling a glacial Lake outburst flood process chain: the case of lake Palcacocha and Huaraz, Peru. *Hydrology and Earth System Sciences 20*, 2519–2543.

Spedding, N. & Evans, D. J. 2002: Sediments and landforms at Kvíárjökull, Southeast Iceland: a reappraisal of the glaciated valley landsystem. *Sedimentary Geology 149*, 21–42.

Stansell, N. D., Polissar, P. J., Abbott, M. B., Bezada, M., Steinman, B. A. & Braun, C. 2014: Proglacial lake sediment records reveal Holocene climate changes in the Venezuelan Andes. *Quaternary Science Reviews 89*, 44–55.

Stansell, N. D., Rodbell, D. T., Abbott, M. B. & Mark, B. G. 2013: Proglacial lake sediment records of Holocene climate change in the western Cordillera of Peru. *Quaternary Science Reviews 70*, 1–14.

Stansell, N. D., Rodbell, D. T., Licciardi, J. M., Sedlak, C. M., Schweinsberg, A. D., Huss, E. G., Delgado, G. M., Zimmerman, S. H. & Finkel, R. 2015: Late glacial and Holocene glacier fluctuations at Nevado Huaguruncho in the eastern Cordillera of the Peruvian Andes. *Geology 43*, 747–750.

Stefaniak, A. M., Robson, B. A., Cook, S. J., Clutterbuck, B., Midgley, N. G. & Labadz, J. C. 2021: Mass balance and surface evolution of the debris-covered Miage Glacier, 1990-2018. *Geomorphology 373*, 107474, https://doi.org/10.1016/j.geomorph.2020.107474.

Stokes, C. R., Tarasov, L., Blomdin, R., Cronin, T. M., Fisher, T. G., Gyllencreutz, R., Hätterstand, C., Heyman, J., Hindmarsh, R. C. A., Hughes, A. L. C., Jakobsson, M., Kirchner, N., Livingstonen, S. J., Margold, M., Murton, J. B., Noormets, R., Peltier, W. R., Peteet, D. M., Piper, D. J. W., Preusser, F., Renssen, H., Roberts, D. H., Rocher, D. M., Saint-Ange, F., Stroven, A. P. & Teller, J. T. 2015: On the reconstruction of palaeo-ice sheets: recent advances and future challenges. *Quaternary Science Reviews 125*, 15–49.

Tacsi Palacios, A., Colonia Ortiz, D., Torres Castillo, J. & Santiago Martel, A. 2014: *Inventario de Lagunas Glaciares del Peru*. 54 pp. Autoridad Nacional del Agua – Unidad de Glaciología y Recursos Hídricos, Huaraz, Perú.

Thomas, E. K. & Briner, J. P. 2009: Climate of the past millennium inferred from varved proglacial lake sediments on Northeast Baffin Island, Arctic Canada. *Journal of Paleolimnology 41*, 209–224.

Torres Amado, L. N., Dávila Roller, L. R. & Vilca Gómez, O. 2016: *Monitoreo Glaciológico en el Glaciar Llaca: Informe Técnico N°03*. 36

pp. Instituto Nacional de Investigación en Glaciares y Ecosistemas de Montaña (INAIGEM), Huaraz, Perú.
Veettil, B. K. 2018: Glacier mapping in the Cordillera Blanca, Peru, tropical Andes, using Sentinel-2 and Landsat data. *Singapore Journal of Tropical Geography 39*, 351–363.
Veettil, B. K., Wang, S., Souza, S. F., Bremer, U. S. & Simões, J. C. 2017: Glacier monitoring and glacier-climate interactions in the tropical Andes: a review. *Journal of South American Earth Sciences 77*, 281–246.
Vilímek, V., Klimeŝ, J. & Červená, L. 2016: Glacier-related landforms and glacial lakes in Huascarán National Park, Peru. *Journal of Maps 12*, 193–202.
Vilímek, V., Zapata, M. L., Klimes, J., Patzel, Z. & Santillán, N. 2005: Influence of glacial retreat on natural hazards of the Palcacocha Lake area, Peru. *Landslides 2*, 107–115.
Viviroli, D., Archer, D. R., Buytaer, W., Fowler, H. J., Greenwood, G. B., Hamlet, A. F., Huang, Y., Koboltsching, G., Litaror, M. I., López-Moreno, J. I., Lorentz, S., Schadler, B., Schreier, H., Schwaiger, K., Vuille, M. & Woods, R. 2011: Climate change and mountain water resources: overview and recommendations for research, management and policy. *Hydrology and Earth System Sciences 15*, 471–504.
Vuille, M., Bradley, R. S., Werner, M. & Keimig, F. 2003: 20th century climate change in the tropical Andes: observations and model results. *Climatic Change 59*, 75–99.
Vuille, M., Carey, M., Huggel, C., Buytaert, W., Rabatel, A., Jacobsen, D., Soruco, A., Villacis, M., Yarleque, C., Elison Timm, O., Condom, T., Salzmann, N. & Sicart, J.-E. 2018: Rapid decline of snow and ice in the tropical Andes – impacts, uncertainties and challenges ahead. *Earth-Science Reviews 176*, 195–213.
Vuille, M., Francou, B., Wagnon, P., Juen, I., Kaser, G., Mark, B. G. & Bradley, R. S. 2008: Climate change and tropical Andean glaciers: past, present and future. *Earth-Science Reviews 89*, 79–96.
Watson, C. S., Quincey, D. J., Carrivick, J. L. & Smith, M. W. 2016: The dynamics of supraglacial ponds in the Everest region, central Himalaya. *Global and Planetary Change 142*, 14–27.
Wegner, S. A. 2014: *Lo que el Agua se Llevó: Consecuencias y Lecciones del Aluvión de Huaraz de 1941 - Nota Técnica 7*. 88 pp. Notas Técnicas sobre Cambio Climático, Ministerio del Ambiente, Lima, Perú.
Wigmore, O. & Mark, B. 2017: Monitoring tropical debris-covered glacier dynamics from high-resolution unmanned aerial vehicle photogrammetry, Cordillera Blanca, Peru. *The Cryosphere 11*, 2463–2480.
Wood, J. L., Harrison, S., Wilson, R., Emmer, A., Yarlenque, C., Glasser, N. F., Torres, J. C., Caballero, A., Araujo, J., Bennet, G. L., Diaz-Moreno, A., Garay, D., Jara, H., Poma, C., Reynolds, J. M., Riveros, C. A., Romero, E., Shannon, S., Tinoco, T., Turpo, E. & Villafane, H. 2021: Contemporary glacial lakes in the Peruvian Andes. *Global and Planetary Change 204*, 103574, https://doi.org/10.1016/j.gloplacha.2021.103574.